Stabilized quantum field theory

C. D. Chlouber*
(Dated: 08/08/24)

This analysis shows that divergence issues in QFT can be resolved without mass and charge renormalization by postulating a two-component theory of the vacuum whose net energy and charge are zero. For the free fields, the quantum vacuum is uniformly homogeneous and isotropic, but interacting fields break the uniformity as vacuum energy is redistributed. For an irreducible self-interaction amplitude Ω, infinite field actions divide the vacuum into positive and negative self-energy components such that the net vacuum energy correction to a scattering process is finite in the presence of external fields, but vanishes for free particles. For each particle mass in a loop, two mass states dressed with vacuum energy, are constructed for fermion and boson self-energy processes. For electroweak interactions, the stabilized amplitude $\hat{\Omega} = \Omega - \overline{\Omega}$ includes a correction for a vacuum energy deficit within an infinitesimal near-field (INF) region, where $\overline{\Omega}$ is given by an average of Ω over dressed mass levels. For QCD, strong interactions redistribute vacuum energy so that there is a surplus in the INF with a corresponding deficit in the surrounding far-field resulting in a sign reversal of $\hat{\Omega}$ relative to QED and asymptotic freedom. Stabilized amplitudes are shown to agree with renormalization for radiative corrections in Abelian and non-Abelian gauge theories.

I. INTRODUCTION

A long-standing enigma in particle physics is how an elementary charged particle such as an electron can be stable in the presence of its own electromagnetic field [1, 2]. Critical accounting for system stability is essential since radiative corrections in quantum field theory (QFT) involve self-interactions that appear to change the mass and charge of a particle. In this analysis we propose a physical mechanism that stabilizes a particle such that its mass and charge retain their physically observed values in radiative processes.

The agreement between renormalization theory and experiment confirms the effect of vacuum fluctuations on the dynamics of elementary particles to astounding accuracy. For example, electron anomalous magnetic moment calculations currently agree with experiment to about 1 part in a trillion [3, 4]. This achievement is the result of more than seven decades of effort since the relativistically invariant form of the theory took shape in the works of Feynman, Schwinger, and Tomonaga; see Dyson's unified account [5, 6]. The agreement leaves little doubt that QFT predictions are correct; however, the renormalization technique [7–9] used to overcome divergence issues in radiative corrections offers little insight into the underlying physics behind charge stability in the high-energy regime. Recall that divergent integrals occur in scattering amplitudes for self-energy processes and arise in sums over intermediate states of arbitrarily high-energy virtual particles. This stymied progress until theoretical improvements were melded with renormalization to isolate the physically significant parts of radiative corrections by absorbing infinities into the electron mass and charge.

Although the renormalization method used to eliminate ultraviolet divergences yields predictions in remarkable agreement with experiments, early investigators including developers of the theory: Dirac, Feynman, and Schwinger [10–13] expressed concerns about the method. Largely due to elegant and persuasive renormalization group arguments [14–16], many workers in the field no longer believe that the divergences in QFT and the renormalization procedure used to overcome them are issues requiring further consideration.

The basic flaw in the theory that is fixed up by renormalization is simply this: Standard QFT does not specify a source for the energy required to create ultrahigh-energy virtual particles in radiative corrections, and the scattering amplitude does not account for the change in that source. Renormalization eliminates the infinities, but it can hardly be regarded as a fundamental solution since it did not identify and address this flaw.

The purpose of this analysis is to develop an alternative to renormalization in QFT for the free and interacting fields. A minimal requirement for this proposal is that it reproduce the successes of the accepted theory: These include the successful higher-order multiloop calculations of quantum electrodynamics (QED), and the modern understanding of QED as a part of non-Abelian electroweak theory [17–19], and asymptotic freedom predictions [20, 21] in quantum chromodynamics (QCD). We define an energetically stable system (charge plus vacuum) and develop a stabilized amplitude applicable to all radiative processes and particles of the Standard Model. Our primary results for electroweak and QCD scattering amplitudes are presented in Sections III C and III D: Scattering matrix corrections for stability

* Houston, USA; dchlouber@okstatealumni.org

are simply constructed using unrenormalized (core) amplitudes from the literature. General arguments are given to demonstrate that net S-matrix corrections in QFT for vacuum polarization, fermion self-energy, and vertex processes are finite and agree with renormalization theory.

II. VACUUM ASSUMPTIONS AND SYNOPSIS

Ordinarily, the vacuum $|0\rangle$ is defined to be the lowest energy state having no observable particles; however, as is well known, it's not empty. From a classical point of view, it's natural to assume that the vacuum is a ground state having zero energy since observed particles have positive energy. Physically, one expects the fermion vacuum $|0_f\rangle$ to be electrically neutral; however, according to Dirac's relativistic electron theory [22], the existence of a stable positive energy electron implies an infinite sea of negative energy electrons, for example. Similarly, the quantized radiation field exhibits an infinite zero-point energy [23] since the field consists of an infinite number of quantum mechanical oscillators, each having a positive ground state energy. At the submicron level, zero-point fluctuations of the radiation field result in an attractive force between closely spaced parallel conducting plates first predicted by Casimir [24, 25], and subsequently confirmed by experiments [26–28]. Although ground state energies are not unexpected in quantum mechanics, an infinite vacuum energy strongly suggests that the theory is missing something. In QFT only energy differences are considered significant, and one can just shift the energy. However, gravity accounts for all mass-energy contributions, and vacuum energy impacts the accelerated expansion of the universe through the cosmological constant. In contrast to calculations for a typical quantum field, astronomical measurements suggest a vacuum energy density of only $4.8\,GeV/m^3$ in the space between galaxies: This is the cosmological constant paradox discussed by Weinberg [29].

Standard QFT eliminates divergent ground state energies by introducing infinite renormalization constants [30, 31]. For the free fields, this is equivalent to a subtraction or a normal ordering of operators in the Hamiltonian and current density [32]: This uniquely defines a vacuum whose net energy and charge vanish. If we suppose that the infinity arising from field quantization and the renormalization constant have physical significance, then the vacuum must include two components for each particle of the Standard Model that oppose one another such that its net energy and charge are zero. For the fermion field this suggests that $|0_f\rangle$ includes positive energy antifermions in addition to Dirac's negative energy sea; similarly for bosons, we have a dual sea of positive energy bosons and negative energy antibosons comprising the boson vacuum $|0_b\rangle$. Since the amplitude to create a negative energy state is zero for both fermions and bosons, negative energy particles are confined to the vacuum and unobservable; see Equations (A10) and (A22) in Appendix A. Ordinary matter exclusive of dark matter and $|0_f\rangle$ form a stable system; for example, a positive energy electron can not annihilate a positron in the vacuum since that would expose (create) a negative energy electron in the Dirac sea for which no observable state exists. While individual vacuum components are infinitely uncertain, the ground state energy of the complete vacuum is certain — it is zero in this physical model in agreement with renormalization of the free fields. In the absence of interactions, the quantum vacuum is assumed to be homogeneous, isotropic, and unique.

The physical resolution of these infinities follows simply from conservation laws. From classical mechanics, any agent or process that does work or creates particles requires a source of energy: Uncompensated infinities in QFT are a direct result of neglecting this basic principle that ensures conservation of energy. Quantization is a process that effectively does work to create a sea of vacuum particles in QFT. For bosons, a positive energy sea is created during quantization of the free fields. The question that must be answered is this: Where did the energy to create this positive energy sea of oscillators come from? Since it is a vacuum energy, and the only known source of an infinite amount of energy is the vacuum, we are compelled to conclude that its source is the vacuum, and there must exist a deficit consisting of negative energy antibosons such that the net energy and charge (for W-bosons) of $|0_b\rangle$ are zero. Similarly, Dirac's sea of charged negative energy fermions is created during quantization, so if we assume that the source of the energy required to create Dirac's sea is the vacuum itself, then there must exist a sea of positive energy antifermions if energy and charge conservation hold. Antifermions are locked up in the vacuum; consequently, they are rare in the observed universe. Therefore, we have a two-component vacuum for both bosons and fermions that has a well-defined physical significance since it is comprised of known particles in the Standard Model (SM). The complete vacuum including all SM particles is defined in Equation (A37).

According to QFT, boundary conditions in the Casimir experiment reduce the number of positive energy radiation modes between the plates. From a mechanical point of view, negative work is done to bring the plates together from infinity, so there must be an opposing positive energy in the region exterior to the plates; therefore, energy is redistributed. The singularity that occurs in the Casimir calculation arises from field quantization, and its subtraction to obtain the finite result of physical interest accounts for the negative energy modes and ensures that the net energy of the vacuum remains zero.

For radiative corrections in QFT, an unrenormalized (core) scattering amplitude corresponding to an irreducible

Feynman diagram contains a finite part of physical interest and a divergent self-energy (SE) part [6, 33, 34]. To isolate the finite part of the amplitude, renormalization introduces counter-terms that eliminate the SE part in the core amplitude such that the net amplitude is finite in the presence of external fields, but vanishes for free particles. The method of counter-terms [35, 36] is equivalent to ultra-near-field mass or charge corrections for fermion and boson self-energy diagrams, respectively.

For an irreducible radiative correction, the desired finite scattering amplitude may be obtained without renormalization by including a correction to the amplitude which represents a self-energy deficit (SED). To create ultrahigh-energy virtual particles in electroweak interactions, for example, charges in radiative corrections borrow energy locally from the vacuum leaving a self-energy deficit (SED). Again, we have two physically significant vacuum components, the borrowed SE and the SED. Vacuum energy is redistributed, but its net energy and charge remain zero.

In summary, quantization of the free fields and radiative corrections are singular processes that create infinite amounts of vacuum energy/charge for which we make the following assumptions:

Assumption 1. The net energy and charge of the vacuum are zero.

Assumption 2. Singular processes in QFT borrow energy/charge from the vacuum leaving a deficit.

III. FORMULATION – INTERACTING FIELDS

Stability conditions, a complete set of mass states including vacuum energy, and stabilized scattering amplitudes are derived for fermions and bosons.

A. Physical model for fermions

Regarding an electron as a point particle [37], the classical electrostatic self-energy $e^2/2a \equiv \alpha\Lambda_\circ$ diverges linearly as the shell radius $a \to 0$, or energy cutoff $\Lambda_\circ \to \infty$, where $-e$ is the charge and $\alpha = e^2/4\pi$ is the fine-structure constant. However, Weisskopf [38, 39] showed using Dirac's theory [22] that charge is effectively dispersed over a region comparable in size to the Compton wavelength of the electron, $\lambda_c\,(m) = 1/m$ in natural units, due to pair creation in the vacuum, and the self-energy only diverges logarithmically. Feynman's calculation [33] in covariant QED yields an electromagnetic mass

$$m_{em}^{+} = \frac{3\alpha m}{2\pi}\left(\ln\frac{\Lambda_\circ}{m} + \frac{1}{4}\right)\,, \tag{1}$$

where $m = g_e v/\sqrt{2}$ is the observed mechanical mass generated via interaction between the fermion and Higgs fields in electroweak theory, g_e is a coupling constant, and v is the ground state vacuum energy. In the absence of a compensating negative energy, equation (1) signals an energetically unstable electron. This is the fermion self-energy (FSE) problem, whose general resolution will suggest a solution for boson self-energy (BSE) processes as well resulting in finite amplitudes for all radiative corrections. In this section we derive a vacuum stability condition and a complete set of mass states for an electron.

Renormalization theory posits that a negatively infinite "bare" mass $m_\circ$ must exist to counterbalance m_{em}^{+} such that the mass infinity is eliminated

$$m_\circ + m_{em}^{+} = m\,. \tag{2}$$

For lack of physical evidence, negative matter is naturally met with some skepticism; see Dirac's discussion [40] of the classical problem, for example. Nevertheless, energies that stabilize a charge must be negative to conserve energy, and we can understand their origin by first considering the source for the electrical energy required to assemble a classical charge from infinitesimal parts in the rest frame. Since the agents that do the work must draw energy $\mathcal{E}_{em}^{+}$ from an external energy source (well), the well's energy is depleted and the total energy

$$\mathcal{E} = m + \mathcal{E}_{em}^{+} + \mathcal{E}_w \tag{3}$$

of the system including matter, electromagnetic field $\mathcal{E}_{em}^{+}$, and energy well $\mathcal{E}_w$ is constant.

Assume that the depleted energy well is part of the vacuum, elementary charges are inherently stable, and consider an electron and its neighboring vacuum as two distinct systems that can act on one another. In particular, we suppose that an electron borrows energy locally from the vacuum to create its electrostatic field with a vacuum energy deficit

$$\mathcal{E}_w \to \mathcal{E}_{em}^- = -\mathcal{E}_{em}^+ \tag{4}$$

located in an infinitesimal near-field (INF) region. This corresponds to a redistribution of vacuum energy into positive and negative energy parts such that equation (3) is satisfied for a free particle; therefore, we have a stability condition

$$m_{em}^+ + m_{em}^- \;=\; 0\,, \tag{5}$$

where $\mathcal{E}_{em}^{\pm} = m_{em}^{\pm}$ in natural units. Thus, an electrically charged particle effectively acts as a sink for negative energy, and the deficit must be taken into account to uphold energy conservation.

In addition to the experimental (core) mass m, equation (5) suggests that a stable electron includes two electromagnetic masses $m_{em}^{\pm}$ that are assumed large in magnitude, but finite, until the final step of the development. We can think of $m_{em}^{\pm}$ as components of an electromagnetic vacuum (zero net energy) which are tightly bound to the core mass and inseparable from the core and each other, at least for finite field actions. From equation (3), either mass can be associated with m. Considering all non-vanishing masses constructed from the set $\{m,\, m_{em}^+,\, m_{em}^-\}$, we define a complete set of mass levels $m + \lambda M$, where $\lambda = \{0,\, \pm 1\}$ and $M \equiv |m_{em}^{\pm}|$. For $\lambda = \pm 1$, an electromagnetically dressed core mass (DCM) refers to a composite particle with mass levels

$$m_d = m + \lambda M\,. \tag{6}$$

For a particle of four-momentum p, the dressed momentum is $p_d = p + \lambda P_M$, where P_M is the momentum of M.

Dressed mass states are important for radiative corrections because they provide additional degrees of freedom needed to compute INF corrections to scattering amplitudes which stabilize the system. Introduction of a bare mass or charge in renormalization theory does not account for all possible mass states in radiative processes; consequently, the underlying physics is concealed, and the theory is rendered more complicated: For example, introducing a bare mass only results in an asymmetry which requires wave field renormalization in the electron self-energy problem.

Consider a free particle state $|p,\, m\rangle$ satisfying $p^2 = m^2$. Spin is omitted in $|p,\, m\rangle$ since it is inessential to the subsequent development, and the rest mass is included because it is the fundamental particle characteristic which becomes dressed with vacuum energy in stability corrections to the S-matrix discussed in Section III C. For radiative corrections, assume that dressed states $|p_d\,,\, m_d\rangle$ may be created with equal probability in intermediate states with infinitesimally small lifetimes $\Delta t \simeq \hbar/\left(m_d c^2\right)$ in accordance with Heisenberg's uncertainty principle [41]. Scattering amplitudes for low-energy processes are unaffected because the energies are insufficient to excite dressed states in $|p_d\,,\, m_d\rangle$. In fact, we will see that finite parts of radiative corrections vanish in the limit $\eta \equiv M/m \to \infty$.

B. General dressed mass states

This section generalizes DCM rules to all elementary particles and radiative processes of the electroweak Standard Model; in particular, we derive a rule for dressing particles in BSE processes with vacuum energy.

External lines for processes in Fig. 1 involve (a) gauge bosons $b \in \{\gamma,\, W,\, Z\,,H\}$, and (b,c) fermions f. Blobs in Fig. 1 contain irreducible insertions, which in general, may involve photons and other particles in the Standard Model mass set

$$\mathbb{M} = \{m_f,\, m_W,\, m_Z,\, m_H\}\ .$$

On the mass shell, scattering amplitudes $\Sigma^f\,(p)$ and $\Sigma^b\left(k^2\right)$ define fermion and boson self-energy functions [42, 43]

$$M_f = \left.\Sigma^f\,(p)\right|_{\not{p}=m_f}\ , \tag{7}$$

$$M_b^2 = \mathrm{Re}\left[\Sigma^b(k^2)\right]_{k^2=m_b^2}\ , \tag{8}$$

where $\not{p} = \gamma^\mu p_\mu$, and γ^μ are Dirac matrices. Masses M_f and M_b are assumed to represent energy borrowed from the vacuum to create a configuration of ultrahigh-energy virtual particles. To account for vacuum depletion and thereby ensure energy and charge conservation, a general correction to the scattering amplitude valid for all three processes in

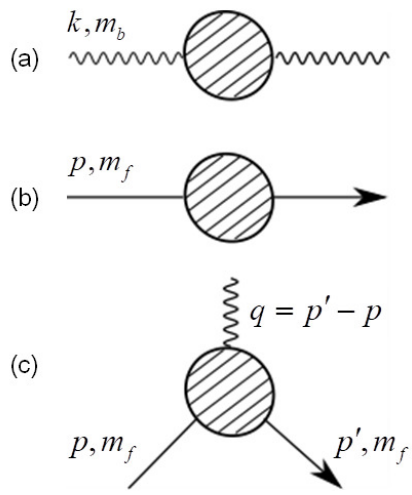

Figure 1. Generic self-energy and vertex diagrams: (a) BSE, (b) FSE, and (c) vertex.

Fig. 1 is required. To define this correction, we notice that equations (7) and (8) suggest additional mass states and Feynman diagrams, where physical particle masses are dressed with vacuum energy as in equation (6) for fermions.

In general, DCM levels for fermions in FSE processes and massive bosons $b \in \{W,\, Z\,, H\}$ in BSE processes are defined by requiring that averages of free field Lagrangian densities over dressed mass levels for each particle class give the undressed value. Since Yukawa and Higgs densities, $\mathcal{L}_{\mathrm{F}}^{\mathrm{Yukawa}}\left(m_f\right)$ and $\mathcal{L}_{\mathrm{H}}\left(m_b^2\right)$ in equations (C17) and (C11), involve sums of terms linear in m_f and m_b^2, we have

$$\frac{1}{2}\sum_{\lambda=\pm 1}\mathcal{L}_F^{Yukawa}\left(m_f+\lambda M_f\right)=\mathcal{L}_F^{Yukawa}\left(m_f\right)\,, \tag{9}$$

$$\frac{1}{2}\sum_{\lambda=\pm 1}\mathcal{L}_H\left(m_b^2+\lambda M_b^2\right)=\mathcal{L}_H\left(m_b^2\right)\,. \tag{10}$$

Defining a common scaling factor η such that $M_f \equiv \eta m_f$ and $M_b \equiv \eta m_b$, dressed masses are generated by

$$m_f \to m_f\left(1+\lambda\eta\right)\,, \tag{11}$$

$$m_b^2 \to m_b^2\left(1+\lambda\eta^2\right)\,. \tag{12}$$

For the purpose of defining general stability corrections for radiative processes, we can focus on the mass dependence of core amplitudes.

To ensure consistency when fermions and bosons mix in FSE and BSE processes, DCM levels for all $m \in \mathbb{M}$ in the blobs of Fig. 1 are defined by the replacement

$$m^n \to m_d^n = m^n\left(1+\lambda\eta^n\right)\,, \tag{13}$$

where $m = m_f|m_b$, and

$$n=\begin{cases}1 & \text{FSE/vertex}\\ 2 & \text{BSE}\end{cases} \tag{14}$$

for irreducible FSE, vertex, and BSE diagrams in electroweak theory. The regulation of infrared singularities for soft photon emissions [33] provides a simple example: For FSE and vertex processes, a fermion m_f and a small photon mass μ mix in terms of form $\ln\frac{m_f}{\mu}$; for consistency, we require

$$\mu \to \mu\left(1+\lambda\eta\right)\,, \tag{15}$$

then $\ln\frac{m_f}{\mu}$ is invariant under (11) and (15). External momenta $\not{p} = m + \delta\not{p}_{os}$ and $k^2 = m^2 + \delta k_{os}^2$ in Fig. 1 become dressed in the blobs

$$\not{p} \to \not{p}_d = m_d + \delta\not{p}_{os}\,, \tag{16}$$

$$k^2 \to k_d^2 = m_d^2 + \delta k_{os}^2\,, \tag{17}$$

where $\delta\not{p}_{os}$ and δk_{os}^2 are off-shell terms which are arbitrary but stationary under (13), and they are zero for free particles. With $\lambda = \pm 1$ in equation (13), (16) and (17) define a complete set of dressed momentum states.

From Appendix C 1, vertex factors in equations (C19)-(C21) including the weak mixing angle (C10), charge (C23), and neutral current coupling constants (C24) are all stationary under (13). However, propagators (C25)-(C27) involving massive particles are not stationary under DCM transforms, and dressed amplitudes (20) constructed from them are either driven to zero or a stabilizing correction for finite tree or divergent loop processes, respectively.

Since $m \propto v$ in Higgs mass formulae, dressed mass levels correspond to vacuum displacements:

$$\Delta v = \lambda \eta v \,, \tag{18}$$

$$\Delta v^2 = \lambda \eta^2 v^2 \tag{19}$$

for FSE and BSE processes; see Appendix C 1 equations (C12)-(C14) and (C18). Averaging over λ, the mean vacuum displacement is zero.

C. Electroweak scattering amplitude

Generally, if an irreducible radiative process represented by Ω borrows energy or charge from the vacuum creating a deficit, then an opposing amplitude is required to account for the deficit. For the moment, assume dimensional regularization is used to tame improper integrals. The total amplitude is defined by

$$\hat{\Omega} = \Omega\left(\mathbb{M}\right) - \overline{\Omega}\left(\mathbb{M}\right) \,, \tag{20}$$

where Ω accounts for self-interaction effects involving physical masses in $\mathbb{M}$, and

$$\overline{\Omega}\left(\mathbb{M}\right) = \frac{1}{2} \lim_{\eta \to \infty} \sum_{\lambda = \pm 1} \Omega\left(\mathbb{M}_d = \eta_\lambda \mathbb{M}\right) \tag{21}$$

is a subtrahend for vacuum depletion that includes all intermediate mass states dressed with vacuum energy; from equations (13) and (14), we have

$$\eta_\lambda \equiv \begin{cases} 1 + \lambda\eta & \text{FSE/vertex} \\ \sqrt{1 + \lambda\eta^2} & \text{BSE} \end{cases} \,. \tag{22}$$

From equation (8), the depletion amplitude $-\overline{\Omega}$ represents a squared mass deficit in $\hat{\Omega}$ for BSE processes. In addition to m_b or m_f, Ω depends on external momenta $\{k, p\}$ for Feynman diagrams in Fig. 1 which may be on- or off-shell. For notational simplicity, any dependence on external momentum parameters has been suppressed during construction of $\overline{\Omega}$ because $\{k, p, q\}$ are implicitly dependent on associated core masses.

In dimensional regularization we have a singular function [44, 45]

$$D\left(\Delta, \sigma\right) = \frac{1}{\sigma} - \ln \Delta - \gamma \,, \tag{23}$$

where $\sigma = 2 - \mathrm{d}/2$ with spacetime dimension $\mathrm{d} \lesssim 4$; Δ depends on $\mathbb{M}$, momentum parameters external to the loop, and integration variables. $\gamma = 0.577\cdots$ is the Euler-Mascheroni constant. Divergent terms involving $1/\sigma$ cancel in equation (20), and the net amplitude is well defined since it involves a factor $-\ln|\Delta/\Delta_\circ|$, where

$$\Delta_\circ = \lim_{\eta \to \infty} \eta_\lambda^{-2} \Delta(\eta_\lambda \mathbb{M}) \tag{24}$$

from equation (D4). Four-momenta in Δ go on-shell upon taking the limit in (24); see equation (D10).

If an energy cutoff $\Lambda_\circ$ is assumed in lieu of dimensional regularization, then we must include $\Lambda_\circ$ in the arguments of Ω. If a particle of mass m probes energies up to $\Lambda_\circ$ in the core amplitude Ω, then a dressed particle with mass

$$m_d = \eta_\lambda m \tag{25}$$

probes energies with cutoff

$$\Lambda_d = \eta_\lambda \Lambda_\circ \,; \tag{26}$$

that is, the cutoff scales in the same way as (25). For FSE/vertex and BSE processes, dressed momenta $\left(p_d, k_d^2\right)$ with cutoffs $\left(\Lambda_d, \Lambda_d^2\right)$ sample all mass states ($\lambda = \pm 1$) in equation (13), and go on on-shell in $\overline{\Omega}$ such that the net amplitude $\hat{\Omega}$ contains only physical masses and finite terms of physical interest for all processes. Cutoff scaling is required for a consistent definition of integrals in Ω and $\overline{\Omega}$: it synchronizes the cutoff to $\Lambda_\circ$, and yields a well defined limit as $\eta \to \infty$ in equation (21). Divergent integrals occurring in Ω and $\overline{\Omega}$ are invariant under equations (25) and (26); for electron self-energy, this is evident from the argument of the logarithm in equation (1), and again, divergent terms in equation (20) cancel.

To obtain physical distances probed in high energy processes, assume $\eta \gg 1$, and take the magnitude

$$|\Lambda_d| \;\approx\; \eta\Lambda_\circ \,, \tag{27}$$

then Ω and $\overline{\Omega}$ probe infinitesimal far-field (IFF) and infinitesimal near-field (INF) distances

$$r_\circ \;\approx\; \Lambda_\circ^{-1} \quad \text{IFF} \,, \tag{28}$$

$$r_d\,(\eta) \;\approx\; r_\circ/\eta \quad \text{INF} \,. \tag{29}$$

Therefore, vacuum energy is redistributed with a surplus in the far-field region $r \geq r_\circ$ and a deficit at the origin $r_d\,(\eta \to \infty) = 0$.

In contrast to the regulator technique of Pauli and Villars [46], the above method employs physically meaningful dressed mass levels, albeit virtual only, and it applies to all radiative processes in QFT without introduction of auxiliary constraints.

From the functional form in equation (21), $\overline{\Omega}$ represents the same basic physical process as Ω, but it is distinguished by sticky collisions between core masses and vacuum energy components. Since $-\overline{\Omega}$ opposes Ω, it represents a negative probability amplitude correction; thus, Feynman's conjecture [11] that negative probabilities might be used " $\cdots$ to solve the original problem of infinities in quantum field theory" appears well founded.

D. QCD scattering amplitude

The foregoing DCM rules apply to QCD as well since its Lagrangian is invariant under an average over dressed mass states. As with electroweak, all vertex factors are independent of mass and are therefore DCM invariant. However, two modifications are required:

First, the sign of $\hat{\Omega}$ must be reversed. Since the Callan-Symanzik [47, 48] beta function depends on coefficients of divergent terms only [49], the sign reversal is expected from opposing signs in the first two terms of equation (23). However, the sign reversal admits a much more enlightening physical interpretation if one assumes, in contrast to an electrical charge, that a color charge redistributes vacuum energy so there is a far-field deficit which is balanced by an INF surplus as depicted in Fig. 2: For an electric or color charge, we have a generalized stability condition

$$\left(\mathcal{E}^+ + \mathcal{E}^-\right)_{vac} = 0 \,. \tag{30}$$

Resulting colored quarks and gluons are enveloped in a negative energy color field which suggests that the quasi-probability of observing them is likewise negative, at least for low energy probes. Since positive and negative energy regions in Fig. 2 for color charges are interchanged relative to electrical charges, the stabilized amplitude in QCD is

$$\hat{\Omega}_{QCD} = \lambda_s \hat{\Omega} \,, \tag{31}$$

where $\hat{\Omega}$ from equation (20) employs the usual Feynman rules, and

$$\lambda_s = -1 \tag{32}$$

is a switching factor. For a physically meaningful interpretation of amplitudes, unobservable quark and gluon states must have negative norm and spacelike momenta.

Second, for gluon self-energy diagrams in the pure gauge sector, we lack a mass reference; a solution is to introduce a small gluon mass μ_g via $k^2 \to k^2 - \mu_g^2$ in gluon propagators when constructing amplitudes. Define

$$m_d^2 = \mu_g^2 + \lambda M_g^2\big|_{\mu_g = 0} \;\; (M_g \equiv \eta\mu_\circ) \;, \tag{33}$$

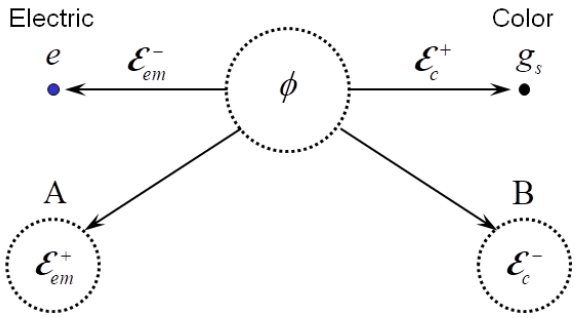

Figure 2. Intrinsically stable electrical and color charges $\{e, g_s\}$ effectively draw {negative, positive} energy from the vacuum ϕ leaving an energy {surplus, deficit} in surrounding (far-field) regions {A, B}.

where M_g is an INF energy surplus, and $\mu_\circ$ is an arbitrary unit of mass measure: $\mu_\circ$ can be related to a standard reference mass M_s, usually chosen to be the Z-boson mass m_Z, such that the polarization function vanishes on the mass shell. An analytic expression

$$M_s = \sqrt{\frac{1}{n_f}\sum_{f=1}^{n_f} m_f^2} \tag{34}$$

is derived in Appendix F; see equation (F31). Evaluating equation (34) for $n_f = 6$ quarks gives $M_s = 70.65\,\mathrm{GeV}/c^2$; compare with $m_Z = 91.1876\,\mathrm{GeV}/c^2$. Introduction of mass terms of the form (33) does not break gauge invariance since the sum over mass levels in the Yang-Mills Lagrangian is zero.

IV. VERIFICATION

This section briefly justifies rules (20) and (31) for computing stabilized amplitudes. The method given below simplifies the determination of finite scattering amplitudes, and it is to be compared with renormalization approaches; see Dyson [6], for example. Refer to Appendix B for a more detailed verification.

A. Electroweak Interactions

For three classes of diagrams in Fig. 1, equation (20) is verified for electroweak processes focusing on mass and momentum external to the loop. An extensive set of Feynman diagrams and expressions for unrenormalized amplitudes is given in [43] and cited references. Results below agree with [43, 50] as shown by a more detailed analysis in Appendix G.

Depletion amplitudes $-\overline{\Omega}$ for diagrams in Fig. 1 meet basic requirements for a vacuum energy deficit: they have negative energy localized at a point (in the limit $\eta \to \infty$), and account for additional mass states (13).

For BSE processes in Fig. 1 (a), equation (20) gives

$$\hat{\Sigma}^b(s) = \Sigma^b(s) - \overline{\Sigma}^b(s)\ , \tag{35}$$

where the dependence on $s = k^2$ in included, and $\mathbb{M}$ is omitted to simplify notation. Applying equation (21), the dressed amplitude

$$\overline{\Sigma}^b(s) = \Sigma^b\left(m_b^2\right) + \left.\frac{\partial \Sigma^b}{\partial s}\right|_{s=m_b^2}\left(s - m_b^2\right) \tag{36}$$

includes only the first two terms of a Taylor series expansion of $\Sigma^b(s)$ after averaging over dressed mass states. In the expansion of $\Sigma^b(s)$, factors involving mass ratios are invariant under equation (13), $s - m_b^2$ is invariant under (17), and dressed higher order derivatives vanish in the limit $\eta \to \infty$. Since equation (35) satisfies expected mass shell conditions [51]

$$\hat{\Sigma}^b\left(m_b^2\right) = 0\,, \tag{37}$$

and

$$\left.\frac{\partial\hat{\Sigma}^{b}\left(s\right)}{\partial s}\right|_{s=m_{b}^{2}}=0\,, \tag{38}$$

it is finite and agrees with renormalization.

For FSE processes in Fig. 1 (b), we have

$$\hat{\Sigma}^{f}\left(p\right)=\Sigma^{f}\left(p\right)-\overline{\Sigma}^{f}\left(p\right)\,. \tag{39}$$

Similarly to (36), the series expansion of $\Sigma^{f}\left(p\right)$ yields a dressed amplitude

$$\overline{\Sigma}^{f}\left(p\right)=\left.\Sigma^{f}\left(p\right)\right|_{\not{p}=m_{f}}+\left.\frac{\partial\Sigma^{f}}{\partial\not{p}}\right|_{\not{p}=m_{f}}\left(\not{p}-m_{f}\right)\,. \tag{40}$$

In the expansion of $\Sigma^{f}\left(p\right)$, $\not{p}-m_{f}$ is invariant under equation (16), and dressed higher order derivatives again vanish in the limit $\eta\rightarrow\infty$. For a free particle

$$\left.\hat{\Sigma}^{f}\left(p\right)\right|_{\not{p}=m_{f}}=0\,, \tag{41}$$

and

$$\left.\frac{d\hat{\Sigma}\left(p\right)}{d\not{p}}\right|_{\not{p}=m_{f}}=0 \tag{42}$$

ensures that $i=\sqrt{-1}$ is the residue of the propagator pole. The second term in equation (40) eliminates any need for wave field renormalization, and equation (39) is indeed the desired finite amplitude.

Equation (20) is easily verified for vertex diagrams in Fig. 1 (c): From Ward's identity [52], the vertex function $\Lambda^{\mu}\left(q\right)$ is dimensionless; consequently, the dressed amplitude $\overline{\Lambda}^{\mu}\left(q\right)$ involves only the first (divergent) term in an expansion of $\Lambda^{\mu}\left(q\right)$ about the origin since $q_{d}=q$, and dressed derivatives vanish as $\eta\rightarrow\infty$. Therefore, $\overline{\Lambda}^{\mu}\left(q\right)=\Lambda^{\mu}\left(0\right)$, and

$$\left.\hat{\Lambda}^{\mu}\left(q\right)\right|_{q=0}=0 \tag{43}$$

in agreement with renormalization.

Equations (37)-(38) for bosons and (41)-(43) for fermions represent free particle vacuum stability conditions for all primitively divergent diagrams.

B. Strong Interactions

For non-Abelian QCD, Appendix F applies equation (31) to one-loop diagrams in Fig. 3. The arguments in Section IV A are general: stabilized QCD amplitudes are finite and agree with asymptotic freedom predictions [49, 53].

Gluon loops (B) and (C) of Fig. 3 generate a clustering of like-gluons; consequently, as one probes a charged gluon cloud, the effective color coupling decreases as expected from QCD anti-screening effects only if $\lambda_{s}=-1$; from equation (F27),

$$\overline{\alpha}_{s}\left(\rho_{s}\right)=\frac{\alpha_{s}}{1-\lambda_{s}\frac{\alpha_{s}}{4\pi}\left(11-\frac{2}{3}n_{f}\right)\ln\rho_{s}}\quad\left(\lambda_{s}=-1\right)\,, \tag{44}$$

where $\alpha_{s}=\frac{g_{s}^{2}}{4\pi}$ is the strong coupling constant, n_{f} is the number of quarks, and $\rho_{s}=-\frac{k^{2}}{M_{s}^{2}}$ with spacelike momentum k.

Gluon loop insertions (B) into the quark/3-gluon vertex (C) of Fig. 3 enhances clustering of like-gluons.

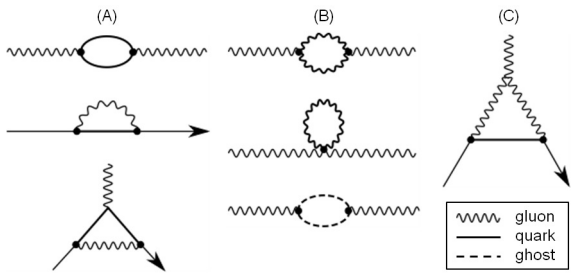

Figure 3. Feynman diagrams for strong interaction processes in QCD: (A) BSE, FSE, and vertex; (B) BSE for gluons in pure gauge sector; and (C) quark/3-gluon vertex. For accretion amplitude $\overline{\Omega}$, particle lines between dots become dressed with vacuum energy.

V. CONCLUSIONS

Evidence presented for QFT supports the hypothesis that singularities redistribute vacuum energy. For the free fields in QFT, renormalization itself together with simple conservation of energy arguments strongly suggest that the quantum vacuum has two opposing components each consisting of known particles in the Standard Model. Quantum field theoretic computations which claim that the zero-point energy of the entire vacuum is non-zero or infinite do not account for the energy of the opposing vacuum component. Antimatter only appears to be rare since it is normally confined to the vacuum along with negative energy matter modes.

Generally, infinite field actions split the vacuum into negative and positive energy components. For radiative corrections involving electroweak or strong interactions, vacuum energy is redistributed such that the sum of the self-energy and self-energy deficit of a free particle is zero. The model was generalized to apply to all Standard Model interactions by defining mass states dressed with both positive and negative vacuum energy for fermion and boson self-energy processes: These new intermediate mass states have infinitesimally short duration and are the key to computing vacuum energy corrections which stabilize the theory. Concise rules for constructing stabilized S-matrix corrections were developed and applied to resolve divergence issues in Abelian QED and non-Abelian QCD and electroweak theories without renormalization.

In strong interactions, the dressed amplitude $\overline{\Omega}$ corresponds to an accretion of vacuum energy in a pointlike near-field interaction region of radius $r \ll \Lambda_\circ^{-1}$, and the physical masses are cloaked in the depletion part $-\Omega$ of the stabilized amplitude. Compared to an electrical charge, a color charge acts on the vacuum to create a field of negative energy surrounding quarks at distances $r \geq \Lambda_\circ^{-1}$. This suggests that particle observability may be a consequence of how charges redistribute vacuum energy. Since negative energy particles are confined to the vacuum and have no observable state, a positive energy quark surrounded by negative vacuum energy may be exceedingly difficult to isolate from its environment which is tantamount to confinement.

For Abelian and non-Abelian theories, the stability method is expected to yield finite results to all orders in perturbation theory since it is applied repeatedly in any complex Feynman diagram to each irreducible radiative correction working from the innermost loop outward; a detailed proof for Abelian QED is given in Appendix E 4.

Infinite mass, charge, and wave-field renormalizations are required in the standard (unstabilized) theory because core amplitudes do not account for the source of energy required to create a configuration of ultrahigh-energy virtual particles; this violates conservation of energy. The infinity in the core amplitude for an irreducible radiative correction represents energy or charge borrowed from the vacuum within limits imposed by Heisenberg's uncertainty principle [41]. In each case, there exists two physically significant vacuum components, the borrowed energy and a deficit, such that the net vacuum energy and charge remain zero. Finite stabilized amplitudes account for the self-energy deficit, agree with renormalized QFT, and are uniquely determined in contrast to multiple renormalization schemes.

Assumptions almost identical to those in Section II have been successfully applied to the gravitational singularity of a black hole to explain the origin of dark matter and dark energy [54]. In this theory, a black hole redistributes vacuum energy by polarizing the vacuum creating a dark matter halo with a uniform background of dark energy.

[1] F. Rohrlich, Am. J. Phys **28**, 639 (1960).
[2] M. Janssen and M. Mecklenburg, in *Interactions* (Springer, 2006) pp. 65–134.
[3] T. Aoyama, M. Hayakawa, T. Kinoshita, and M. Nio, Phys. Rev. D **85**, 093013 (2012).
[4] D. Hanneke, S. Fogwell Hoogerheide, and G. Gabrielse, Phys. Rev. A **83**, 052122 (2011).
[5] F. J. Dyson, Phys. Rev. **75**, 486 (1949).
[6] F. J. Dyson, Phys. Rev. **75**, 1736 (1949).
[7] H. A. Bethe, Phys. Rev. **72**, 339 (1947).
[8] S. S. Schweber, H. A. Bethe, and F. de Hoffmann, *Mesons and Fields*, Vol. I (Row, Peterson and Co., 1955) Ch. 21a discusses H. A. Kramer's mass renormalization principle. See Ch. 21e for polarization tensor factorization.
[9] H. A. Kramers, in *Shelter Island Conference. See Ch. 21 in S. S. Schweber, H. A. Bethe, and F. de Hoffmann, Mesons and Fields, Vol. I (Row, Peterson and Co., Evanston, 1955)* (1947) see Ch. 21 in S. S. Schweber, H. A. Bethe, and F. de Hoffmann, *Mesons and Fields*, Vol. I (Row, Peterson and Co., Evanston, 1955).
[10] J. Schwinger, Phys. Rev. **82**, 914 (1951).
[11] R. P. Feynman, in *Quantum Implications: Essays in Honour of David Bohm*, edited by F. D. Peat and B. Hiley (Routledge & Kegan Paul Ltd, London & New York, 1987) pp. 235–248.
[12] P. A. M. Dirac, Scientific American **208**, 45 (1963).
[13] H. Kragh, *Dirac: a scientific biography* (Cambridge University Press, 1990).
[14] M. Gell-Mann and F. E. Low, Phys. Rev. **95**, 1300 (1954).
[15] N. Bogoliubov and D. V. Shirkov, *Introduction to the Theory of Quantized Fields* (Interscience, New York, 1959).
[16] K. G. Wilson, Rev. Mod. Phys. **55**, 583 (1983).
[17] S. L. Glashow, Nucl. Phys. B **22**, 579 (1961).
[18] S. Weinberg, Phys. Rev. Lett. **19**, 1264 (1967).
[19] A. Salam, in *Elementary Particle Theory*, edited by N. Svartholm (New York : Wiley – Stockholm : Almqvist and Wiksell, 1968).
[20] H. D. Politzer, Phys. Rev. Lett. **30**, 1346 (1973).
[21] D. J. Gross and F. Wilczek, Phys. Rev. Lett. **30**, 1343 (1973).
[22] P. A. M. Dirac, Proc. R. Soc. London, Ser. A **117**, 610 (1928).
[23] P. Jordan and W. Pauli, Z. Physik **47**, 151 (1928).
[24] H. B. G. Casimir, Proc. Kon. Ned. Akad. Wet. **51**, 793 (1948).
[25] E. Lifshitz, JETP **2**, 73 (1956).
[26] M. Sparnaay, Nature **180**, 334 (1957).
[27] S. K. Lamoreaux, Phys. Rev. Lett. **78**, 5 (1997).
[28] M. Bordag, U. Mohideen, and V. M. Mostepanenko, Physics Reports **353**, 1 (2001).
[29] S. Weinberg, Rev. Mod. Phys. **61**, 1 (1989).
[30] A. I. Miller, *Early quantum electrodynamics: A sourcebook* (Cambridge University Press, 1995).
[31] J. Schwinger, *Selected papers on quantum electrodynamics* (Courier Corporation, 1958).
[32] G. C. Wick, Phys. Rev. **80**, 268 (1950).
[33] R. P. Feynman, Phys. Rev. **76**, 769 (1949).
[34] J. M. Jauch and F. Rohrlich, *The Theory of Photons and Electrons* (Springer-Verlag, New York, 1976) Ch. 9-10, App. A5-2, Supp. S2.
[35] N. Bogoliubov and D. Shirkov, *Introduction to the Theory of Quantized Fields* (Wiley, New York, 1980).
[36] I. J. Aitchison, *An informal introduction to gauge field theories* (CUP Archive, 1982) sec. 8.1.
[37] L. D. Landau and E. M. Lifshitz, *The Classical Theory of Fields* (Pergamon, Oxford, 1975) Sec. 15.
[38] V. F. Weisskopf, Z. Angew. Phys. **89**, 27 (1934), english translation given in A. I. Miller, *Early Quantum Electrodynamics: A Source Book* (Cambridge U. Press, New York, 1994).
[39] V. F. Weisskopf, Phys. Rev. **56**, 72 (1939).
[40] P. A. M. Dirac, Proc. R. Soc. London, Ser. A **167**, 148 (1938).
[41] W. Heisenberg, Zeitschrift für Physik **43**, 172 (1927).
[42] A. Sirlin, Phys. Rev. D **22**, 971 (1980).
[43] W. F. Hollik, Fortschr. Phys. **38**, 165 (1990).
[44] G. 't Hooft and M. Veltman, Nucl. Phys. B **44**, 189 (1972).
[45] F. Mandl and G. Shaw, *Quantum Field Theory* (Wiley, New York, 1984) pp. 188, 227, 231.
[46] W. Pauli and F. Villars, Rev. Mod. Phys. **21**, 434 (1949).
[47] C. G. Callan, Phys. Rev. D **2**, 1541 (1970).
[48] K. Symanzik, Commun. Math. Phys. **18**, 227 (1970).
[49] D. J. Gross and F. Wilczek, Phys. Rev. D **8**, 3633 (1973).
[50] A. Denner, Fortschr. Phys. **41**, 307 (1993).
[51] M. E. Peskin and D. V. Schroeder, *An Introduction to Quantum Field Theory* (Addison-Wesley, New York, 1995) p. 332ff, Sec. 16, A.4.
[52] J. C. Ward, Proc. Phys. Society **A64**, 54 (1951).
[53] H. D. Politzer, Physics Reports **14**, 129 (1974).

[54] C. D. Chlouber, "Vacuum energy redistribution in a cyclic universe of black holes," (2024), doi: 10.5281/zenodo.12660047.
[55] L. Canetti, M. Drewes, and M. Shaposhnikov, New J Phys **14**, 095012 (2012).
[56] W. Pauli and V. Weisskopf, Helv Phys Acta **7**, 709 (1934).
[57] P. Jordan and E. P. Wigner, Z. Phys **47**, 14 (1928).
[58] V. Fock, Z. Physik **75**, 622 (1932).
[59] P. A. M. Dirac, in *Report to 7th Solvay Conference* (1933).
[60] J. Schwinger, Phys. Rev. **75**, 651 (1949).
[61] W. Heisenberg, Zeitschrift für Physik **90**, 209 (1934).
[62] W. Heisenberg, Zeitschrift fur Physik **92**, 692 (1934).
[63] G. Gamow, Physical Review **70**, 572 (1946).
[64] R. A. Alpher, H. Bethe, and G. Gamow, Phys. Rev. **73**, 803 (1948).
[65] The AMS Collaboration, Physics Reports **894**, 1 (2021).
[66] G. Dissertori, "The Determination of the Strong Coupling Constant," (The Standard Theory of Particle Physics, 2016) Chap. 6, pp. 113–128.
[67] M. Böhm, H. Spiesberger, and W. Hollik, Fortschritte Der Physik **34**, 687 (1986).
[68] P. W. Higgs, Phys. Rev. Lett. **13**, 508 (1964).
[69] M. Tanabashi *et al.*, Phys. Rev. D **98**, 030001 (2018).
[70] R. P. Feynman, Phys. Rev. **76**, 749 (1949).
[71] G. 't Hooft and M. Veltman, Nucl. Phys. B **50**, 318 (1972).
[72] M. Gell-Mann, M. L. Goldberger, and W. Thirring, Phys. Rev. **95**, 1612 (1954).
[73] R. E. Cutkosky, J. Math. Phys. **1**, 429 (1960).
[74] G. Källén, Helv. Phys. Acta. **25**, 417 (1952).
[75] J. D. Bjorken and S. D. Drell, *Relativistic Quantum Mechanics* (McGraw-Hill, New York, 1964) p. 163.
[76] J. Schwinger, Phys. Rev. **73**, 416 (1948).
[77] H. M. Foley and P. Kusch, Phys. Rev. **73**, 412 (1948).
[78] S. Weinberg, Phys. Rev. **118**, 838 (1960).
[79] A. Salam, Phys. Rev. **82**, 217 (1951).
[80] G. Källén and A. Sabry, Dan. Mat. Fys. Medd. **29**, 1 (1955).
[81] G. 't Hooft, Nucl. Phys. B **35**, 167 (1971).
[82] G. Passarino and M. Veltman, Nucl. Phys. B **160**, 151 (1979).
[83] G. 't Hooft and M. Veltman, Nucl. Phys. B **153**, 365 (1979).
[84] D. A. Ross and J. C. Taylor, Nucl. Phys. B **51**, 125 (1973).
[85] Y. Nagashima, *Elementary Particle Physics: Foundations of the Standard Model*, Vol. 2 (Wiley, 2013) Sec. 5.2.2.
[86] T. Kinoshita and A. Sirlin, Phys. Rev. **113**, 1652 (1959).
[87] M. Roos and A. Sirlin, Nucl. Phys. B **29**, 296 (1971).
[88] T. van Ritbergen and R. G. Stuart, Nucl. Phys. B **564**, 343 (2000).
[89] M. Steinhauser and T. Seidensticker, Phys. Lett. B **467**, 271 (1999).
[90] A. Pak and A. Czarnecki, Phys. Rev. Lett. **100**, 241807 (2008).
[91] W. Hollik, Journal of Physics: Conference Series **53**, 7 (2006).
[92] C. D. Chlouber, "Electroweak: Generate stabilized electroweak polarization profiles," Zenodo (2024), doi: 10.5281/zenodo.12786316.
[93] G. Källén, *Quantum Electrodynamics* (Springer-Verlag, New York, 1972) p. 149.

Appendix A: Two Component Quantum Vacuum

From physical assumptions in Section II, the vacuum consists of two components, a borrowed energy and an energy deficit, that oppose one another such that its net energy vanishes. This appendix defines the vacuum in QFT for the free boson and fermion fields without appealing to renormalization, and it addresses the matter-antimatter asymmetry problem [55]. In a nutshell, any process that creates something out of nothing without an opposing process violates conservation laws for energy, charge, or both.

1. Bosons

To achieve the desired physical result simply, we neglect polarizations and begin with the Klein-Gordon field. For scalar bosons having mass μ, the Hamiltonian for the free field is [23]

$$H_b^+ = \sum_{\overrightarrow{k}} \hbar\omega_k N(k) + \mathscr{E}_{vac}^+ , \tag{A1}$$

where

$$k = \left(k_\circ, \overrightarrow{k}\right) \quad \left(k_\circ = \frac{\omega_k}{c}\right)$$

is a four-wave-vector for a real particle with energy

$$\hbar\omega_k = \sqrt{\left(\hbar\overrightarrow{k}\right)^2 + (\mu c^2)^2} , \tag{A2}$$

$$N(k) = a^\dagger(k)\, a(k)$$

is the number operator, $a(k)$ and $a^\dagger(k)$ are annihilation and creation operators, and

$$\mathscr{E}_{vac}^+ = \frac{1}{2}\sum_{\overrightarrow{k}} \hbar\omega_k \tag{A3}$$

is the zero-point energy; here after, natural units are assumed: $\hbar = c = 1$. Upon quantizing the theory, positive energy vacuum modes in Equation (A3) are created leaving a vacuum energy deficit

$$\mathscr{E}_{vac}^- = -\mathscr{E}_{vac}^+ \tag{A4}$$

according to Assumption 2. The total Hamiltonian

$$H_b = H_b^+ + \mathscr{E}_{vac}^- \tag{A5}$$

is finite, and its vacuum expectation satisfies

$$\langle 0|\, H_b\, |0\rangle = 0 . \tag{A6}$$

For the complex Klein-Gordon field [56], we have a conserved charge associated with the field and particle-antiparticle pairs. Again we have a ground state energy (A3) and vacuum deficit (A4). However, in this case if the $\mathscr{E}_{vac}^+$ component has negative charge, the $\mathscr{E}_{vac}^-$ component must have positive charge. For vector bosons, suppose we generate a sea of negatively charged positive energy W^- bosons from quantization; at a minimum, we need a positively charged negative energy sea W^+ to satisfy Equation (A6) and conserve charge when the field is quantized. Therefore, assume that the general boson vacuum

$$|0_b\rangle = \left|b_+, \bar{b}_-\right\rangle \tag{A7}$$

includes two components: positive energy bosons b_+ and negative energy antibosons $\bar{b}_-$. Negative energy antibosons are not observed and must remain hidden in the vacuum; in consequence, the vacuum is conventionally defined by

$$a(k)\,|0_b\rangle = 0 . \tag{A8}$$

Assuming that the destruction of a particle with momentum k is equivalent to the creation of a negative energy antiparticle with momentum $-k$

$$a\left(k\right) \leftrightarrow \overline{a}^{\dagger}\left(-k\right) \ , \tag{A9}$$

the amplitude

$$\overline{a}^{\dagger}\left(-k\right)\left|0_{b}\right\rangle = 0 \tag{A10}$$

to create an observable negative energy antiparticle is zero. Conversely, the creation of a particle with momentum k is equivalent to the destruction of an antiparticle of opposing momentum $-k$ in $\overline{b}_{-}$

$$a^{\dagger}\left(k\right) \leftrightarrow \overline{a}\left(-k\right) \ ; \tag{A11}$$

therefore, we can construct an observable boson state in two ways

$$\left|k\right\rangle = a^{\dagger}\left(k\right)\left|0_{b}\right\rangle \tag{A12}$$

$$= \bar{a}\left(-k\right)\left|0_{b}\right\rangle \ . \tag{A13}$$

Substituting Equations (A9) and (A11) in the commutation relation

$$\left[a\left(k\right), a^{\dagger}\left(k'\right)\right] = \delta_{kk'} \ , \tag{A14}$$

and setting the discrete $k' = k$, we have

$$\left\langle 0_{b}\right| \left[\overline{a}^{\dagger}\left(-k\right), \overline{a}\left(-k\right)\right] \left|0_{b}\right\rangle = 1 \ . \tag{A15}$$

Taking into account Equation (A10), we see that all the negative energy antiboson states are occupied in agreement with Equation (A7) since Equation (A15) reduces to

$$\left\langle 0_{b}\right| \overline{N}\left(-k\right)\left|0_{b}\right\rangle = 1 \ , \tag{A16}$$

where

$$\overline{N}\left(-k\right) \equiv \overline{a}^{\dagger}\left(-k\right)\overline{a}\left(-k\right)$$

is the number operator for negative energy antiparticles.

2. Fermions

Upon quantization the Hamiltonian [57–59]

$$H_{f}^{-} = \sum_{\overrightarrow{p},s} E_{p}\left[N_{s}\left(p\right) + \overline{N}_{s}\left(p\right) - 1\right] \tag{A17}$$

for the free Dirac field ψ, including the ground state energy, is given by a sum over field excitations with four-momentum $p = (E_{p}, \overrightarrow{p})$ and spin index $s = \pm 1$, where

$$E_{p} = \sqrt{\overrightarrow{p}^{2} + m^{2}} \ ,$$

m is the particle mass,

$$N_{s}\left(p\right) = b_{s}^{\dagger}\left(p\right) b_{s}\left(p\right) \ ,$$

$$\overline{N}_{s}\left(p\right) = \overline{b}_{s}^{\dagger}\left(p\right) \overline{b}_{s}\left(p\right)$$

are number operators for charged fermions and antifermions, and the particle operators obey anticommutation relations

$$\left\{b_{r}\left(p\right), b_{s}^{\dagger}\left(q\right)\right\} = \delta_{pq}\delta_{rs} \ , \tag{A18}$$

$$\left\{\overline{b}_{r}\left(p\right), \overline{b}_{s}^{\dagger}\left(q\right)\right\} = \delta_{pq}\delta_{rs} \ . \tag{A19}$$

To preclude observable negative energy states, the fermion vacuum $|0_f\rangle$ must satisfy

$$b_s(p)\,|0_f\rangle = 0\,; \tag{A20}$$

for antifermions, we have

$$\overline{b}_s(p)\,|0_f\rangle = 0 \tag{A21}$$

and the equivalent constraint

$$b^{\dagger}_{-s}(-p)\,|0_f\rangle = 0\,. \tag{A22}$$

Since negative energy fermion states are forbidden by (A22), but present in the observable (A17), we conclude that H_f^- is incomplete.

Standard Dirac theory is symmetric in real particles and antiparticles, and laboratory experiments seem to substantiate this symmetry since particles and antiparticles are always created and annihilated in pairs. However, if one defines the fermion vacuum as an assembly of equal numbers of negative energy fermions and positive energy antifermions, then the symmetry is broken: We have

$$|0_f\rangle = \left|f_-, \overline{f}_+\right\rangle\,, \tag{A23}$$

where f_- is the usual Dirac sea, and $\overline{f}_+$ is a sea of positive energy antifermions. The fermion vacuum $|0_f\rangle$ is assumed stable and unique at least for electrons and positrons, for example. In Dirac's theory, $\overline{N}_s(p)$ counts holes in f_-, but neglects the bulk of antiparticles in $\overline{f}_+$.

To account for the energy of the companion sea $\overline{f}_+$, we supplement H_f^- with a Hamiltonian for the antifermion sea

$$H_{fc}^{+} \equiv \int \overline{\psi}_c^{\,-}(x)\left(-i\overrightarrow{\gamma}\cdot\overrightarrow{\nabla} + m\right)\psi_c^{+}(x)\,d^3x\,, \tag{A24}$$

where $\psi_c^+(x)$ and $\overline{\psi}_c^{\,-}(x)$ are the positive and negative frequency parts of charge conjugate field ψ_c, $\overline{\psi}_c = \psi_c^{\dagger}\beta$, and $\gamma^{\mu} = (\beta, \overrightarrow{\gamma})$ is a four-vector of Dirac matrices. Utilizing the expansion

$$\psi_c^{+}(x) = \sum_{\overrightarrow{p},s}\sqrt{\frac{m}{VE_p}}c_s(p)\,u_s(\overrightarrow{p})\,e^{-ipx}\,, \tag{A25}$$

involving spinors $u_s(\overrightarrow{p})$, Equation (A24) reduces to

$$H_{fc}^{+} = \sum_{\overrightarrow{p},s} E_p N_s^c(p)\,, \tag{A26}$$

where the occupation number

$$N_s^c(p) = c_s^{\dagger}(p)\,c_s(p) \equiv 1\,,$$

and the complete Hamiltonian

$$H_f = H_f^- + H_{fc}^+ \tag{A27}$$

is finite and counts observable particles only. For example, when a negative energy electron in f_- is excited into a positive energy state, the hole in f_- exposes an already existing positron in $\overline{f}_+$. The negative vacuum energy in (A17) arises from field quantization, and the positive energy vacuum modes in Equation (A26) are required to conserve energy and charge.

To complete the argument, we note that the absence of an antifermion in $|0_f\rangle$ would expose a negative energy fermion of opposite spin, but that is precluded by Equation (A22). However, upon substituting

$$\begin{aligned}\overline{b}_r(p) &\rightarrow b^{\dagger}_{-s}(-p)\,,\\ \overline{b}^{\dagger}_s(q) &\rightarrow b_{-s}(-p)\end{aligned}$$

into anticommutation relation (A19) and taking into account (A22), the vacuum expectation

$$\langle 0_f|\left\{b^{\dagger}_{-s}(-p)\,, b_{-s}(-p)\right\}|0_f\rangle = 1\,. \tag{A28}$$

reduces to

$$\langle 0_f | \, N_{-s} \left(-p \right) | 0_f \rangle = 1 \, ; \tag{A29}$$

where

$$N_{-s} \left(-p \right) \equiv b_{-s}^{\dagger} \left(-p \right) , b_{-s} \left(-p \right) \tag{A30}$$

is the number operator. Therefore, all the negative energy fermion states are occupied in agreement with (A23), but unobservable.

From physical consideration of Equation (A23), we expect that infinite vacuum currents will cancel as well: Defining the antifermion vacuum current by

$$\begin{aligned} j_c^{\mu} \left(x \right) &= e \langle 0_f | \, \overline{\psi}_c^{-} \left(x \right) \gamma^{\mu} \psi_c^{+} \left(x \right) | 0_f \rangle \\ &= e \left\{ \overline{\psi}_c^{-} \left(x \right) , \gamma^{\mu} \psi_c^{+} \left(x \right) \right\} \end{aligned} \tag{A31}$$

and using the anticommutation relations [45, 60]

$$\left\{ \psi_c^{+} \left(x \right) , \overline{\psi_c^{-}} \left(y \right) \right\} = i S^{+} \left(z = x - y \right) \, , \tag{A32}$$

$$\left\{ \psi^{-} \left(x \right) , \overline{\psi}^{+} \left(y \right) \right\} = i S^{-} \left(z \right) \, , \tag{A33}$$

the net current

$$\begin{aligned} j^{\mu} \left(x \right) &= j_c^{\mu} \left(x \right) - e \overline{\psi} \left(x \right) \gamma^{\mu} \psi \left(x \right) \\ &= -e \mathrm{N} \left(\overline{\psi} \left(x \right) \gamma^{\mu} \psi \left(x \right) \right) + e \, \mathrm{tr} \left[\gamma^{\mu} S^{(1)} \left(0 \right) \right] \\ &= -e \mathrm{N} \left(\overline{\psi} \left(x \right) \gamma^{\mu} \psi \left(x \right) \right) \end{aligned} \tag{A34}$$

reduces to Wick's normal product [32], where $S^{\pm} \left(x \right)$ are singular functions for the Dirac field ψ,

$$S^{(1)} \left(z \right) = i \left[S^{+} \left(z \right) - S^{-} \left(z \right) \right] \, ,$$

and the second term in line 2 of (A34) vanishes since $S^{(1)} \left(0 \right) \propto I$ (the identity matrix), and the Dirac matrix is traceless. Therefore, vacuum expectations for the net energy

$$\langle 0_f | \, H_f \, | 0_f \rangle = 0 \tag{A35}$$

and current density

$$\langle 0_f | \, j^{\mu} \left(x \right) | 0_f \rangle = 0 \tag{A36}$$

vanish without ad hoc renormalizations. Schwinger [60] also obtained Equation (A36) using Heisenberg's commutator [61, 62] for the current

$$j^{\mu} = -e \, \left[\overline{\psi} \left(x \right) , \gamma^{\mu} \psi \left(x \right) \right] / 2 \, ,$$

but that definition does not pin point the asymmetry between matter and antimatter as do Equations (A23) and (A34).

The two-component fermion vacuum is consistent with the absence of significant antimatter in the known universe; normally, positive energy antimatter is locked up in the vacuum in this model. Antimatter is only observed in significant quantities when high energy processes create particle-antiparticle pairs; for example, in the hot plasma of the early universe [63, 64], where the vacuum may be completely ionized. If we suppose that the amount of matter exceeds that of antimatter in the hot plasma; then when the plasma cooled, antimatter relaxed into the stable vacuum leaving the original excess of matter over antimatter. The Alpha Magnetic Spectrometer (AMS) experiment [65] is being used to determine the abundance of antimatter in the universe; so far, significant antimatter has not been detected.

3. Conclusions

From current experimental results and the foregoing vacuum models, we conclude that vacua (A7) and (A23) are necessary conditions that conserve energy and charge. The density of negative energy is assumed spatially uniform since negative energy particles in the vacuum can not form stationary modes, but positive energy modes may be excluded from a region by boundary conditions in the Casimir experimental setup, for example. The net energy and charge of the complete vacuum

$$|0\rangle = \prod_{b,f} |0_b\rangle \, |0_f\rangle \ , \tag{A37}$$

including all particles of the Standard Model, vanishes. With respect to energy, the state of the vacuum takes the simple form

$$|0\rangle = \left| \mathscr{E}_{vac}^{+}, \mathscr{E}_{vac}^{-} \right\rangle \ , \tag{A38}$$

where the net vacuum energy

$$\mathscr{E}_{vac} = \mathscr{E}_{vac}^{+} + \mathscr{E}_{vac}^{-} \tag{A39}$$

vanishes.

Vacuum energy may be spatially redistributed via several mechanisms including elementary electrical and color charges plus Casimir effects: $\mathscr{E}_{vac} = 0$ is assumed to hold for all cases. No contribution to the cosmological constant is expected from elementary charges or Casimir effects since vacuum energy is only redistributed locally.

Appendix B: Detailed Verification

The main purpose of this appendix is to show that the stability method agrees with renormalization theory and therefore with experiment for specific radiative corrections in QFT; in particular, rules (20) and (31) for computing stabilized amplitudes in QED, QCD, and electroweak theories are verified. Standard Model nomenclature is defined in Appendix C.

In Appendix D, we evaluate divergent integrals in $\overline{\Omega}$ for dressed mass states in Feynman diagrams, and show how they reduce to mass shell renormalization conditions.

For Abelian QED in Appendix E, stabilized amplitudes agree with renormalization theory for vacuum polarization, fermion self-energy, and vertex processes to all orders in perturbation theory. Accounting for vacuum depletion eliminates all divergences: In particular, opposing currents associated with dressed fermion states stabilize the photon self-energy without charge renormalization, and neither mass nor wave field renormalization is required for the fermion self-energy.

For non-Abelian QCD in Appendix F, we apply the stability method to a collection of one-loop diagrams using a modified renormalization formula to derive an effective color charge (F14) and running coupling constant (F27) with an energy scale signature consistent with QCD's prediction of asymptotic freedom [49, 53] and its agreement with experimental results [66]. However, the crucial difference is that finite stabilization parameters replace infinite renormalization constants. The results show that the switching factor $\lambda_s = -1$ in (F14) is essential; physically, this means that dressed particles in $\overline{\Omega}$ are associated with positive energy in the infinitesimal near-field, and physical masses in the depletion part $-\Omega$ are cloaked in negative energy in the infinitesimal far-field. Also, an analytical expression for the reference mass M_s in QCD is derived which gives $M_s = 70.65\, GeV/c^2$; see (F31).

Generally, fundamental couplings are well defined only on the mass shell, where bosons mediating the interaction are free, and stabilized boson self-energy functions vanish; therefore, the elementary charge used in the Feynman rules is a rock-solid constant. An effective running coupling includes energy dependent vacuum polarization effects for screening or anti-screening, which can otherwise can be associated with modifications to field propagation functions.

For one-loop electroweak corrections in Appendix G, we verify that stabilized boson self-energy corrections including Δr, fermion self-energies, and vertex processes are finite and agree with renormalization [43, 50]. Electroweak depletion amplitudes for boson and fermion self-energy processes are reduced by expanding core amplitudes in a Taylor series and applying (21): The resulting stabilized amplitudes (G14) and (G39) are unique and yield stability conditions that agree with only one renormalization scheme. While the electrical charge (C23) is invariable according to (G29), couplings $\left\{ g_W^2,\, g_Z^2 \right\}$ and θ_W can vary due to finite on-shell mass shifts $\left\{ \delta m_W^2,\, \delta m_Z^2 \right\}$ derived from stabilized $W-$ and $Z-$boson self-energy corrections; see (G53) and (G54). Therefore, resulting Δr corrections (G30) to BSE amplitudes

for $W-$ and $Z-$bosons are a simple consequence of the constancy of the electrical charge, a stability result. Finally, we verify that muon decay with Δr corrections yields expected results without renormalization.

For non-Abelian electroweak and QCD theories, the stability method is expected to yield finite results to all orders in perturbation theory since it is applied to each irreducible radiative correction in any complex Feynman diagram.

Numerical results are presented in Appendix G 6 for electroweak boson and fermion self-energy profiles. Stabilized results for $\gamma - Z$ mixing, $Z-$boson, and $W-$boson polarization profiles differ from and update those given in [43, 67].

Appendix C: Standard Model nomenclature

This appendix summarizes required machinery of the Standard Model utilizing references [43, 51]. Natural units are assumed; that is, $\hbar = c = 1$.

1. Electroweak theory

The electroweak Lagrangian

$$\mathcal{L}_{EW} = \mathcal{L}_{\mathrm{G}} + \mathcal{L}_{\mathrm{H}} + \mathcal{L}_{\mathrm{F}} \tag{C1}$$

for the physical particles includes gauge, Higgs, and fermion parts. Gauge fixing and ghost terms are omitted in (C1) since it is only necessary to consider physical particles for this development. The gauge part, based on a Yang-Mills prototype (C29), is given by

$$\mathcal{L}_{\mathrm{G}} = -\frac{1}{4} W^a_{\mu\nu} W^{a,\mu\nu} - \frac{1}{4} B_{\mu\nu} B^{\mu\nu} \,, \tag{C2}$$

where the field strength tensors

$$\begin{aligned} W^a_{\mu\nu} &= \partial_\mu W^a_\nu - \partial_\nu W^a_\mu + g_W \varepsilon_{abc} W^b_\mu W^c_\nu \,, \\ B_{\mu\nu} &= \partial_\mu B_\nu - \partial_\nu B_\mu \end{aligned} \tag{C3}$$

are expressed in terms of derivatives of the gauge fields: a triplet W^a_μ, $a = 1, 2, 3$ of vector bosons and a singlet B_μ which transform according to $SU(2)$ and $U(1)$ symmetry groups [17], respectively. In (C3), g_W is the non-Abelian SU(2) gauge coupling constant, and ε_{abc} is the Levi-Civita tensor representing the structure constants of $SU(2)$.

The Higgs part is given by

$$\mathcal{L}_{\mathrm{H}} = \left(D_\mu \Phi\right)^\dagger \left(D^\mu \Phi\right) - V\left(\Phi\right) \,, \tag{C4}$$

where

$$\Phi\left(x\right) = \frac{1}{\sqrt{2}} \begin{pmatrix} 0 \\ v + h(x) \end{pmatrix} \tag{C5}$$

is an isospin doublet in a unitary gauge, $h\left(x\right)$ is the real Higgs field which fluctuates about a vacuum $v = \sqrt{-\frac{\mu_\Phi^2}{\lambda_\Phi}}$,

$$V\left(\Phi\right) = \mu_\Phi^2 \Phi^\dagger \Phi + \lambda_\Phi \left(\Phi^\dagger \Phi\right)^2 \tag{C6}$$

is the Higgs potential, that with $\lambda_\Phi > 0$ and $\mu_\Phi^2 < 0$ for symmetry breaking, leads to the stable ground state (C5). The Higgs doublet Φ is coupled to the gauge fields via the covariant derivative

$$D_\mu = \partial_\mu - i g_W T_a W^a_\mu - i g_B \frac{Y}{2} B_\mu \,, \tag{C7}$$

where $\overrightarrow{T} = \overrightarrow{\sigma}/2$ are weak isospin generators, $\overrightarrow{\sigma}$ are Pauli matrices satisfying the SU(2) algebra $[\sigma_i, \sigma_j] = 2i\varepsilon_{ijk}\sigma_k$, and g_B is the Abelian coupling constant. Φ carries hypercharge $Y = Y_\Phi \equiv 1$ and a third component of isospin $T_3\Phi = -\frac{1}{2}\Phi$. In terms of the gauge fields, the physical fields for charged $W-$bosons, neutral Z, and photon A_μ are

$$W^\pm_\mu = \frac{1}{\sqrt{2}} \left(W^1_\mu \mp W^2_\mu\right) \,, \tag{C8}$$

$$\begin{pmatrix} Z_\mu \\ A_\mu \end{pmatrix} = \begin{pmatrix} \cos\theta_W & \sin\theta_W \\ -\sin\theta_W & \cos\theta_W \end{pmatrix} \begin{pmatrix} W^3_\mu \\ B_\mu \end{pmatrix} , \tag{C9}$$

where the weak mixing angle θ_W is defined by

$$\begin{aligned} \cos\theta_W &= \frac{g_W}{g_Z} \\ &= \frac{m_W}{m_Z} , \end{aligned} \tag{C10}$$

where $g_Z = \sqrt{g_W^2 + g_B^2}$. Omitting higher-order non-mass terms, the Higgs part expressed in terms of the physical fields is given by

$$\mathcal{L}_{\rm H} \simeq \frac{1}{2}\partial_\mu h\, \partial^\mu h + m_W^2 W_\mu^- W^{+\mu} + \frac{1}{2} m_Z^2 Z_\mu Z^\mu - \frac{1}{2} m_H^2 h^2 , \tag{C11}$$

where

$$m_W = \frac{1}{2} g_W v , \tag{C12}$$

$$m_Z = \frac{1}{2} g_Z\, v \tag{C13}$$

are vector boson masses generated via the Higgs mechanism [18, 19, 68]. The scalar boson mass (Higgs) is

$$m_H^2 = 2\lambda_\Phi v^2 , \tag{C14}$$

where the quartic self-interaction parameter λ_Φ may be determined using the identity

$$v^2 = \frac{m_W^2 \sin^2\theta_W}{\sqrt{\pi\alpha}} \tag{C15}$$

and experimental values [69] for m_W, $\sin^2\theta_W$, and m_H.

Suppressing the color attribute for quarks, the fermion part of the Lagrangian is given by

$$\mathcal{L}_F = \sum_j \overline{\psi}_L^j i\gamma^\mu D_\mu \psi_L^j + \sum_{j\sigma} \overline{\psi}_R^{j\sigma} i\gamma^\mu D_\mu \psi_R^{j\sigma} + \mathcal{L}_{\rm F}^{\rm Yukawa} \tag{C16}$$

for each lepton or quark doublet (j), where γ^μ are Dirac matrices,

$$\psi_L^j = \begin{pmatrix} \psi_L^{j+} \\ \psi_L^{j-} \end{pmatrix}$$

is a left-handed fermion doublet with component index $\sigma = \pm$, and $\psi_R^{j\sigma}$ is a right-handed singlet for a fermion f indexed by $j\sigma$. The Yukawa interaction part of $\mathcal{L}_F$ is given by a sum of terms

$$\begin{aligned} \mathcal{L}_{\rm F}^{\rm Yukawa}(m_{j\sigma}) &= g_{j\sigma}\left[\left(\overline{\psi}_L^j \Phi\right)\psi_R^{j\sigma} + \overline{\psi}_R^{j\sigma}\left(\Phi^\dagger \psi_L^j\right)\right] \\ &= -m_{j\sigma}\left[\overline{\psi}_L^{j-}\psi_R^{j\sigma} + \overline{\psi}_R^{j\sigma}\psi_L^{j-}\right] , \end{aligned} \tag{C17}$$

where $g_{j\sigma}$ are coupling constants, and masses generated from the interaction between the fermion and Higgs fields are

$$m_{j\sigma} = \frac{1}{\sqrt{2}} g_{j\sigma}\,(v+h)\Big|_{h=0} . \tag{C18}$$

We will also need vertex factors and propagators below for later reference; these, along with propagators for the Higgs, ghost fields, and vertex factors for $SU(N)$ theories may be found in the literature and [51]. For fermions coupling to the W, Z, and γ; vertex factors are

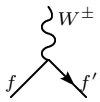

$$= i\frac{e}{\sqrt{2}\,s_w}\gamma^\mu\frac{1}{2}\left(1-\gamma_5\right)\,, \tag{C19}$$

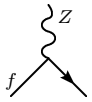

$$= ie\gamma^\mu\left(v_f - a_f\gamma_5\right)\,, \tag{C20}$$

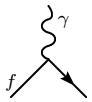

$$= ieQ\gamma^\mu\,, \tag{C21}$$

where ($f = j\sigma\,,\ \sigma = \pm\,,\ f' = j\sigma'\,,\ \sigma' = \mp$), charge operator Q is defined by the Gell-Mann-Nishijima relation

$$Q = T_3 + \frac{Y}{2} \tag{C22}$$

with third component of isospin T_3 and hypercharge Y specific to the fermion, electrical charge e satisfies

$$e \equiv g_W \sin\theta_W = g_B \cos\theta_W\,, \tag{C23}$$

and the vector and axial vector coefficients

$$\begin{aligned} v_f &= \frac{T_3^f - 2s_w^2 Q}{2s_w c_w}\,, \\ a_f &= \frac{T_3^f}{2s_w c_w} \end{aligned} \tag{C24}$$

are neutral current (NC) coupling constants with $\{s_w \equiv \sin\theta_W\,,\ c_w \equiv \cos\theta_W\}$.

The fermion propagator [70] is

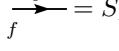

$$= S_F\left(p, m_f\right) = \frac{i}{\not{p} - m_f + i\varepsilon}\,, \tag{C25}$$

where $\not{p} = \gamma^\mu p_\mu$, and anti-fermions are denoted by $\bar{f}$. The vector boson propagator is

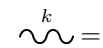

$$= D_F^{\alpha\beta}(k) = \frac{-ig^{\alpha\beta}}{k^2 - m_b^2 + i\varepsilon} \tag{C26}$$

in the Feynman-'t Hooft gauge [71], where the metric tensor $g_{\alpha\beta} = g^{\alpha\beta}$ has non-zero components

$$g_{00} = -g_{11} = -g_{22} = -g_{33} = 1\,,$$

and $b \in \{W,\, Z,\, \gamma\}$. For the Higgs, we have

$$= \frac{i}{k^2 - m_H^2 + i\varepsilon}\,. \tag{C27}$$

Finally, unphysical particles including gauge fixing Higgs $\{\phi^\pm, \chi\}$ and unitarity preserving Faddeev-Popov ghosts $\left\{u^\pm, u^Z, u^\gamma\right\}$ occur in loop corrections discussed in Appendix G.

2. QCD theory

Quantum Chromodynamics is a Yang-Mills theory involving $n_f = 6$ quarks interacting with $n_g = 8$ massless gluons. Quarks carry color charge and belong to the fundamental representation of the color group $G = SU(3)$, and the gluons

are in the adjoint representation $r = G$. Omitting gauge fixing and Faddeev-Popov ghost terms, the QCD Lagrangian is

$$\begin{aligned} \mathcal{L}_{QCD} &= \sum_{f=1}^{n_f} \bar{\psi}_f^j \left(i\gamma_\mu D_{jk}^\mu - m_f \delta_{jk} \right) \psi_f^k + \mathcal{L}_{YM} \,, \\ D_{jk}^\mu &= \delta_{jk} \partial^\mu - i g_s \left(\overrightarrow{t} \cdot \overrightarrow{A}^\mu \right)_{jk} \,, \end{aligned} \tag{C28}$$

$$\begin{aligned} \mathcal{L}_{YM} &= -\frac{1}{4} F_{\mu\nu}^a F_a^{\mu\nu} \,, \\ F_{\mu\nu}^a &= \partial_\mu A_\nu^a - \partial_\nu A_\mu^a + g_s f^{\,abc} A_\mu^b A_\nu^c \,, \end{aligned} \tag{C29}$$

where ψ_f^k is a Dirac spinor for the quark field with flavor f and color state $k \in \{R, G, B\}$, g_s is the color charge, $t^{\,a} = \lambda^a/2\,, a = 1, \ldots, n_g$ are generators represented by 3×3 Gell-Mann matrices λ^a, A_μ^a are color-charged gluon fields, and $f^{\,abc}$ are structure constants of G. The t-matrices, which occur in a quark/gluon vertex

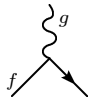

$$= i g_s \gamma^\mu t^a \,, \tag{C30}$$

rotate the quark in color space and generate the Lie algebra for G

$$\left[t^{\,a},\, t^{\,b} \right] = i f^{\,abc} t^{\,c} \,. \tag{C31}$$

The structure constants occur in three- and four-gauge-boson vertices and satisfy

$$f^{\,acd} f^{\,bcd} = C_2\,(G)\, \delta^{ab} \,, \tag{C32}$$

where $C_2\,(G) = N$ is an eigenvalue of the quadratic Casimir operator. The gluon propagator is

$$\underset{a,\mu}{\overset{k}{\sim\!\sim}}\underset{b,\nu}{} = \frac{-i g^{\mu\nu} \delta_{ab}}{k^2 + i\varepsilon} \,. \tag{C33}$$

Appendix D: Divergent integrals

Here we develop integration formulae required for evaluation of stability corrections using cutoff and dimensional regularization. In the p-representation, loop diagrams involve four-dimensional integrals over momentum space, and the real parts of scattering amplitudes contain integrals of the form [34]

$$D\,(\Delta) = \frac{1}{i\pi^2} \int \frac{d^4 p}{\left(p^2 - \Delta\right)^n} = \frac{(-1)^n}{\pi^2} \int \frac{d^4 p_\varepsilon}{\left(p_\varepsilon^2 + \Delta\right)^n} \,, \tag{D1}$$

where Δ depends on the core mass m, momentum parameters external to the loop, and integration variables. On the right side of (D1), a Wick rotation has been performed via a change of variables $p = (i p_\varepsilon^\circ, \vec{p}_\varepsilon)$, so that the integration can be performed in Euclidean space where $p_\varepsilon^2 = p_\varepsilon^\circ p_\varepsilon^\circ + \vec{p}_\varepsilon \cdot \vec{p}_\varepsilon$. Integrals for the divergent case ($n = 2$) must be regulated such that they are consistently defined for core and dressed core masses. For m, D is regularized using a cutoff $\Lambda_\circ$ on $s = |p_\varepsilon|$. In four-dimensional polar coordinates, we have

$$D\,(\Delta, \Lambda_\circ) = \frac{1}{\pi^2} \int d\Omega \int_0^{\Lambda_\circ} ds\, \frac{s^3}{\left[s^2 + \Delta\right]^2} \,. \tag{D2}$$

For dressed masses, Δ depends on m_d, and the domain of integration in equation (D2) must be scaled according to (26); consequently, we need to evaluate

$$D_d = D\left[\Delta\left(m_d\right),\, \Lambda_d\right] \,.$$

With a change of variables $s = \eta_\lambda t$ and taking the limit $\eta \to \infty$, we obtain

$$D_d = D\left(\Delta_\circ, \Lambda_\circ\right) \,, \tag{D3}$$

where

$$\Delta_\circ = \lim_{\eta\to\infty} \eta_\lambda^{-2} \Delta(\eta_\lambda m) \,. \tag{D4}$$

For example, the standard divergent integral [34]

$$\begin{aligned} D_\circ &\equiv D\left(\Delta = m^2, \Lambda_\circ\right) \\ &= \ln \frac{\Lambda_\circ^2}{m^2} - 1 + O\left(\frac{m^2}{\Lambda_\circ^2}\right) \end{aligned} \tag{D5}$$

is manifestly invariant under scaling rules (25) and (26); that is,

$$D_\circ = D\left(m_d^2, \Lambda_d\right) \,. \tag{D6}$$

Note that the average of equation (1) over dressed masses is stationary due to (D6); this ensures that the FSE in QED is finite as shown in detail in Appendix E 2.

In contrast to the cutoff method, dimensional regularization evaluates a Feynman diagram as an analytic function of spacetime dimension d. For $n = 2$ and $d^4p \to d^{\mathrm{d}}p$ in (D1), D may be evaluated using [44, 45]

$$\begin{aligned} D\left(\Delta, \sigma\right) &= \pi^{-\sigma} \Gamma\left(\sigma\right) \Delta^{-\sigma} \\ &= \frac{1}{\sigma} - \ln \Delta - \gamma + O\left(\sigma\right) \,, \end{aligned} \tag{D7}$$

where $\sigma = 2 - \mathrm{d}/2$, and $\gamma = 0.577\cdots$ is the Euler-Mascheroni constant. For $\sigma \neq 0$, the limit $\Lambda_\circ \to \infty$ may be taken since σ regulates the integral. For dressed particles, D_d must yield consistent results for both cutoff and dimensional regularization methods. Considering the requirements used to derive (D3) and employing appendix formulae in [44], we conclude

$$D_d = D\left(\Delta_\circ, \sigma\right) \,. \tag{D8}$$

For the processes in Fig. 1, the argument Δ in (D7) has the form

$$\Delta\left(m, \mu\right) = a m^2 + b \ell^2 + c \mu^2 \,, \tag{D9}$$

where $m = m_b | m_f$, $\ell^2 = k^2 \,|\, p^2 |\, q^2$, $\{a,\, b,\, c\}$ depend on Feynman parameters, and $c = 0$ for BSE processes. Applying equation (D4) to (D9) taking into account (16) and (17), the momenta go on-shell upon computing $\lim\limits_{\eta\to\infty} \eta_\lambda^{-2} \ell_d^2$; that is,

$$\begin{array}{ll} k^2 \to m_b^2 & \text{BSE} \\ p^2 \to m_f^2 & \text{FSE} \\ q^2 \to 0 & \text{Vertex} \end{array} \,, \tag{D10}$$

which we recognize as on-shell renormalization conditions. For the vertex, the dressed momentum transfer is

$$\begin{aligned} q_d &= q + \lambda \left(P'_M - P_M\right) \\ &= q \,, \end{aligned} \tag{D11}$$

where P_M is momentum of M, and $\not{P}_M = M$; therefore, $\lim\limits_{\eta\to\infty} \eta_\lambda^{-2} q_d^2 = 0$. The case where particle masses internal and external to the blob in Fig. 1 (a) are both zero occurs for BSE processes in the pure-gauge sector of QCD. For this case, where $\Delta = b k^2$, choose $a = 1$ and introduce a small gluon mass $m \to \mu_g$, then using (F9), evaluate

$$\Delta_\circ = \lim_{\eta\to\infty} \eta_\lambda^{-2} \Delta\left(\eta_\lambda \mu_\circ\right) = \mu_\circ^2 \tag{D12}$$

with $\eta_\lambda = \sqrt{\lambda}\,\eta$. Thus for all $m \geq 0$, the net S-matrix amplitude computed from (20) is well defined since it involves a factor

$$\frac{\Gamma(\sigma)}{\Delta^\sigma} - \frac{\Gamma(\sigma)}{\Delta_\circ^\sigma} = -\ln\left|\frac{\Delta}{\Delta_\circ}\right| . \tag{D13}$$

The second term on the left side of (D13) is associated with an opposing vacuum energy required for system stability. In addition to a divergent part, $\overline{\Omega}$ in (21) may include a finite part, a constant, that cancels a like term in Ω.

Appendix E: QED verification

Let us apply the foregoing theory with integration formulae given above to verify that net amplitudes for second order radiative corrections in Abelian QED are convergent and agree with results obtained via renormalization. Cutoff and dimensional regularization approaches are used to illustrate the method.

1. Vacuum polarization

The photon self-energy associated with Fig. 4 (a) results in a propagator modification [6]

$$D_F'^{\alpha\beta} = D_F^{\alpha\beta} + D_F^{\alpha\mu}\left(i\hat{\Pi}_{\mu\nu}\right) D_F^{\nu\beta} , \tag{E1}$$

where

$$\hat{\Pi}_{\mu\nu} \equiv \Pi_{\mu\nu} - \overline{\Pi}_{\mu\nu}$$

is a polarization tensor generalized to include the stability correction, and

$$\Pi_{\mu\nu}(k,\, m) = -\frac{ie^2}{(2\pi)^4}\int d^4p\, \mathrm{tr}\left[\gamma_\mu S_F(p,m)\gamma_\nu S_F(p-k,m)\right] \tag{E2}$$

follows from the Feynman-Dyson rules [5, 33]. In consequence of Lorentz and gauge invariance [8] or by direct calculation, it factors into

$$\Pi_{\mu\nu}(k,\, m) = \Pi\left(k^2,\, m^2\right)\left(g_{\mu\nu}k^2 - k_\mu k_\nu\right) . \tag{E3}$$

As is well known, the contribution from terms $k_\mu k_\nu$ vanishes due to current conservation upon connection to an external fermion line. For a massless photon, k^2 is invariant under a DCM transform, and we need only focus on the scalar function $\Pi\left(k^2, m^2\right)$.

Since the scattering amplitude is in general a complex analytic function, it follows from Cauchy's formula that the real and imaginary parts are related by a dispersion relation [72]. The imaginary part is divergence free and may be obtained by replacing Feynman propagators with cut propagators on the mass shell according to Cutkosky's cutting rule [73] or, alternatively, via calculation in the Heisenberg representation as shown in [74]. In particular for vacuum polarization, the real part is given by

$$\Pi\left(k^2,\, m^2\right) = \frac{1}{\pi}\int_{4m^2}^{4\Lambda_\circ^2} ds\, \frac{g\left(\frac{4m^2}{s}\right)}{s - k^2} \tag{E4}$$

with imaginary part

$$g(w) = -\frac{\alpha}{3}\sqrt{1-w}\,(1 + w/2) .$$

Applying (21) using (25) and (26) and performing a change of variables $s = \left(1 + \lambda\eta^2\right)t$ in (E4), we have

$$\begin{aligned}\overline{\Pi} &= \frac{1}{2}\lim_{\eta\to\infty}\sum_{\lambda=\pm1}\Pi\left(k^2,\, m^2 + \lambda\eta^2 m^2\right) \\ &= \frac{1}{2\pi}\lim_{\eta\to\infty}\sum_{\lambda=\pm1}\int_{4m^2}^{4\Lambda_\circ^2} dt\, \frac{g\left(\frac{4m^2}{t}\right)}{t - \left(1+\lambda\eta^2\right)^{-1}k^2} .\end{aligned} \tag{E5}$$

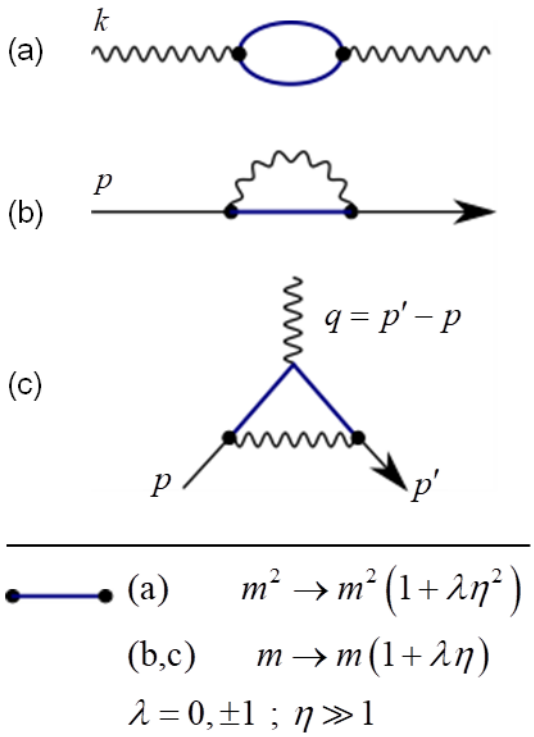

Figure 4. Baseline radiative corrections in QED: (a) photon self-energy, (b) fermion self-energy, and (c) vertex involve the core mass only in internal fermion lines. Two additional diagrams, obtained by replacing the core mass with electromagnetically dressed mass levels, are required for each radiative process to account for vacuum depletion and ensure stability.

Letting $\eta \to \infty$, we see that (E5) is equivalent to a core amplitude evaluated on the light cone

$$\overline{\Pi} = \Pi(k^2 = 0,\, m^2)\,. \tag{E6}$$

Combining (E4) and (E5), we obtain a once-subtracted dispersion relation

$$\begin{aligned} \hat{\Pi}\left(k^2\right) &= \Pi\left(k^2,\, m^2\right) - \Pi\left(0,\, m^2\right) \\ &= \frac{k^2}{\pi}\int_{4m^2}^{\infty} ds\, \frac{g\left(\frac{4m^2}{s}\right)}{s\left(s-k^2\right)} \end{aligned} \tag{E7}$$

in agreement with renormalized QED. For massless photons, $\hat{\Pi}\left(0\right) = 0$ represents a stability condition for vacuum polarization.

For an infinite sum of 1PI insertions, the generalized photon propagator is

$$= -\frac{ig_{\mu\nu}}{k^2}\hat{Z}_3\left(k^2\right)\,, \tag{E8}$$

where the finite stabilization parameter

$$\hat{Z}_3\left(k^2\right) = \frac{1}{1-\hat{\Pi}\left(k^2\right)} \tag{E9}$$

modifies the free photon propagator. Alternatively, one can define a running coupling constant

$$\alpha\left(k^2\right) = \hat{Z}_3\left(k^2\right)\alpha_\circ\,; \tag{E10}$$

in this interpretation, the measured $\left(\alpha_\circ = \frac{e^2}{4\pi}\right)$ and effective couplings are equivalent on the light cone

$$\hat{Z}_3\left(0\right) = 1\,. \tag{E11}$$

Since a stationary state for a photon only exists on the light cone, the fundamental coupling is well defined there, and the stabilized photon self-energy vanishes.

In terms of an external current $j_\mu^{ext}\left(x\right)$, the observable current is given by

$$j_\mu^{obs}\left(x\right) = j_\mu^{ext}\left(x\right) + \delta j_\mu\left(x\right)\,, \tag{E12}$$

where

$$\delta j_\mu\left(x\right) = \frac{1}{\left(2\pi\right)^4}\int d^4k\, e^{ikx} j_\mu^{ext}\left(k\right)\left[\Pi(k^2) - \Pi(0)\right] \tag{E13}$$

is the induced current. In standard renormalization theory (SRT), the last term in brackets is associated with a correction to a divergent bare charge ($e_\circ$), but here, we assert that the correction is a stability requirement associated with opposing vacuum currents involving dressed fermions in the loop. Physical and bare charges in SRT are related by

$$e^2 = \left(Z_3 = \frac{1}{1 - \Pi\left(0,\, m^2\right)}\right) e_\circ^2\,, \tag{E14}$$

where $\sqrt{Z_3}$ is the charge renormalization constant. Charge renormalization in SRT is a consequence of neglecting vacuum depletion in violation of the law of conservation of energy.

2. Fermion self-energy

The fermion self-energy operator corresponding to the Feynman diagram in Fig. 4 (b) is

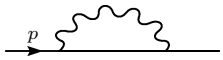

$$= -i\Sigma\left(p, m\right)\,, \tag{E15}$$

where

$$\Sigma\left(p, m\right) = -\frac{e^2}{\left(2\pi\right)^4}\int d^4k\, \gamma_\mu\, S_F\left(p - k, m\right)\, \gamma^\mu \frac{1}{k^2 - \mu^2}\,. \tag{E16}$$

After standard reduction and dimensional regularization, Σ simplifies to

$$\Sigma\left(p, m\right) = \frac{\alpha}{2\pi}\left\{S_1 + \int_0^1 dx\, \left[2m - \not{p}x + \sigma\left(\not{p}x - m\right)\right]\, D\left(\Delta, \sigma\right)\right\}\,, \tag{E17}$$

where $D\left(\Delta, \sigma\right)$ is given by equation (D7) with

$$\Delta = \left(1 - x\right)\left(m^2 - xp^2\right) + x\mu^2\,.$$

The integral expression in equation (E17) is equivalent to a form given in [51], while the term

$$S_1 = -\frac{1 - \sigma}{4}\not{p}$$

follows from appendix formulae in [34] and represents a surface contribution arising from a term linear in k during reduction of equation (E16).

Evaluation of $\overline{\Sigma}$ using (21) reduces to negating equation (E17) and replacing $\Delta \to \Delta_\circ$ according to equation (D8); we obtain

$$\overline{\Sigma}\left(p, m\right) = \frac{\alpha}{2\pi}\left\{S_1 + \int_0^1 dx\, \left[2m - \not{p}x + \sigma\left(\not{p}x - m\right)\right]\, D\left(\Delta_\circ, \sigma\right)\right\}\,, \tag{E18}$$

where

$$\Delta_\circ = m^2 (1-x)^2 + x\mu^2$$

follows from equation (D10). Terms involving $[(\lambda P_M, \lambda M)\ ;\ M = \eta m]$ have canceled in the average over DCM levels yielding a function of the observable mass and momentum only. The net correction, including all three mass levels in Fig. 4 (b), is given by (cf. [33])

$$\begin{aligned} \hat{\Sigma}(p) &= \Sigma - \overline{\Sigma} \\ &= \frac{\alpha}{2\pi} \int_0^1 dx\ (2m - \not{p} x) \ln \left[\frac{m^2 (1-x)^2 + x\mu^2}{(m^2 - xp^2)(1-x) + x\mu^2} \right] , \end{aligned} \tag{E19}$$

where the limit $\sigma \to 0$ has been taken to recover four-dimensional spacetime. With a change of variables $x = 1 - z$, equation (E19) is seen to be identical to the renormalized result given in [75].

The processes in Fig. 4 (b), including iterations in the series

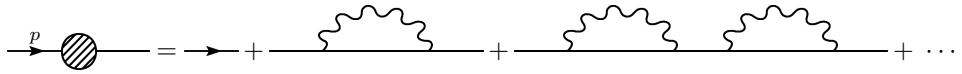

(E20)

yields a modified propagator [5, 6]

$$\begin{aligned} S'_F &= S_F + S_F \left(-i\hat{\Sigma}(p) \right) S'_F \\ &= \frac{i}{\not{p} - m - \hat{\Sigma}(p) + i\varepsilon} , \end{aligned} \tag{E21}$$

which has the desired pole at $\not{p} = m$ since equation (E19) vanishes on the mass shell

$$\hat{\Sigma}(p)\Big|_{p^2 = m^2} = 0 . \tag{E22}$$

Using the general expression for the stabilized fermion self-energy

$$\hat{\Sigma}(p) = \Sigma(p) - \Sigma(m) - \left. \frac{\partial \Sigma}{\partial \not{p}} \right|_{\not{p} = m} (\not{p} - m) , \tag{E23}$$

which is derived in Appendix G 2, we see that

$$\left. \frac{d\hat{\Sigma}(p)}{d\not{p}} \right|_{\not{p} = m} = 0 , \tag{E24}$$

and the residue of the propagator pole is $i = \sqrt{-1}$. For later use, we write equation (E21) in the form

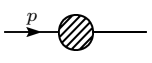

$$= \frac{i}{\not{p} - m + i\varepsilon} \hat{Z}_2(\not{p}) , \tag{E25}$$

where

$$\hat{Z}_2 \equiv \left(1 - \frac{\hat{\Sigma}(\not{p})}{\not{p} - m + i\varepsilon} \right)^{-1} \tag{E26}$$

is a finite stabilization parameter modifying the free field fermion propagator, and is analogous to the renormalization constant Z_2 in SRT relating the bare and renormalized fields via $\psi_\circ = \sqrt{Z_2}\psi$.

Upon identifying

$$m^+_{em} = \Sigma(\not{p} = m,\ \mu = 0) , \tag{E27}$$

$$m^-_{em} = -\overline{\Sigma}(\not{p} = m,\ \mu = 0) , \tag{E28}$$

we see that equation (E22) is equivalent to the FSE stability condition (5). Reverting to cutoff $\Lambda_\circ$ using equation (D1), it follows that (E27) reduces to Feynman's result (1).

In the language of renormalization theory, the bare mass $m_\circ$ in the propagator [45]

$$S'_F = \frac{i}{\not{p} - m_\circ - \Sigma + i\varepsilon} \tag{E29}$$

must be renormalized using (2) with (E27); moreover, wave-field renormalization is required.

3. Vertex

A second-order correction to a corner (C21) involves a replacement

$$ie\gamma^\mu \to ie\Gamma^\mu \,, \tag{E30}$$

where

$$\begin{aligned} \Gamma^\mu &= \gamma^\mu + \Lambda^\mu \\ &= \gamma^\mu F_1\left(q^2\right) + \frac{i\sigma^{\mu\nu}q_\nu}{2m} F_2\left(q^2\right) \,, \end{aligned} \tag{E31}$$

and $\sigma^{\mu\nu} = \frac{i}{2}\left[\gamma^\mu, \gamma^\nu\right]$ are spin matrices. Complete expressions for the form factors F_1 and F_2 can be found in [51]. For small q^2, the vertex function Λ^μ for $\lambda = 0$ in Fig. 4 (c) is given by the approximation [33]

$$\Lambda^\mu\left(q, m\right) = \gamma^\mu L + a^{(2)}\frac{i\sigma^{\mu\nu}q_\nu}{2m} + O\left(\frac{q^2}{m^2}\right) \,, \tag{E32}$$

where

$$L = \frac{\alpha}{4\pi}\left(D_\circ + \frac{11}{2} - 4\ln\frac{m}{\mu}\right) \tag{E33}$$

is a divergent constant. Note that $L = \frac{\alpha}{2\pi}r$, where r is given by equation (23) in [33]. The coefficient $a^{(2)} = \frac{\alpha}{2\pi}$ is the second-order contribution to the anomalous magnetic moment first derived by Schwinger [76] and verified experimentally by [77].

Inserting equation (E32) into (21), using

$$\mu \to \mu\left(1 + \lambda\eta\right) \,, \tag{E34}$$

and accounting for the invariance of $D_\circ$ (D6) under scaling rules (25) and (26), the depletion correction is

$$\overline{\Lambda}^{\,\mu} = \gamma^\mu L \,, \tag{E35}$$

where finite terms in equation (E32) of order $O\left(\frac{q}{m}\right)$ involving replacements

$$m \to m\left(1 + \lambda\eta\right)$$

vanish in the limit $\eta \to \infty$ as we argued in Appendix D; therefore, the total vertex function

$$\hat{\Lambda}^\mu\left(q\right) = \Lambda^\mu - \overline{\Lambda}^{\,\mu} \tag{E36}$$

is convergent, and Λ^μ satisfies the usual renormalization condition for a vertex

$$\hat{\Lambda}^\mu\Big|_{q^2=0, \not{p}=\not{p}'=m} = 0 \,. \tag{E37}$$

This completes verification that lowest-order S-matrix corrections are finite without renormalization.

4. Generalization to higher orders

Our next task is to show that stabilized higher-order radiative corrections in QED are finite and agree with renormalization. The proof closely follows arguments in references cited below and [34]; therefore, we keep our remarks brief highlighting required modifications and differences of interpretation.

Irreducible (skeleton) diagrams include second-order self-energy (SE) and vertex (V) parts discussed above plus infinitely many higher-order primitively divergent V-parts. Using Dyson's expansion method [6], second-order SE- and V-part operators for the core mass are

$$\Sigma = mA - (\not{p} - m)\, B + \hat{\Sigma}\,, \tag{E38}$$

$$\Pi = C + \hat{\Pi}\,, \tag{E39}$$

$$\Lambda^{\mu} = \gamma^{\mu} L + \hat{\Lambda}^{\mu}\,, \tag{E40}$$

where $\{A,\, B\,, C\,,\, L\}$ are logarithmically divergent coefficients depending on $D_{\circ}$. Higher-order primitively divergent V-parts are also of the form (E40) since the degree of divergence [6, 78]

$$K = 4 - \frac{3}{2} f_e - b_e$$

is zero (logarithmic), where $f_e\,(b_e)$ are the number of external fermion (boson) lines; in this case, $L\,(D_{\circ})$ is a power series in α.

Applying equation (21) with (D6), we have

$$\overline{\Sigma} = mA - (\not{p} - m)\, B\,, \tag{E41}$$

$$\overline{\Pi} = C\,, \text{and} \tag{E42}$$

$$\overline{\Lambda}^{\mu} = \gamma^{\mu} L\,, \tag{E43}$$

then stabilized second-order amplitudes (E7), (E19), and (E36)

$$\hat{\Sigma}\left(p^2 = m^2\right) = 0\,, \tag{E44}$$

$$\hat{\Pi}\left(k^2 = 0\right) = 0\,, \tag{E45}$$

$$\hat{\Lambda}^{\mu}\left(q^2 = 0\right) = 0 \tag{E46}$$

vanish on the mass shell. In renormalization theory, the term involving B in equation (E38) is eliminated by wave field renormalization. Higher-order primitively divergent V-parts also satisfy equation (E46) since dressed stabilized amplitudes vanish for on-shell conditions. In this way, equation (20) yields unique finite results

$$\hat{\Sigma} = \Sigma - \overline{\Sigma}\,, \tag{E47}$$

$$\hat{\Pi} = \Pi - \overline{\Pi}\,, \tag{E48}$$

$$\hat{\Lambda}^{\mu} = \Lambda^{\mu} - \overline{\Lambda}^{\mu} \tag{E49}$$

for all irreducible diagrams; therefore, SE-part insertions

$$S_F \;\rightarrow\; S_F + S_F\left(-i\hat{\Sigma}\right) S_F\,, \tag{E50}$$

$$D_F^{\alpha\beta} \;\rightarrow\; D_F^{\alpha\beta} + D_F^{\alpha\mu}\left(i g_{\mu\nu} k^2 \hat{\Pi}\right) D_F^{\nu\beta} \tag{E51}$$

into lines, and V-part insertions

$$\gamma^{\mu} \rightarrow \gamma^{\mu} + \hat{\Lambda}^{\mu} \tag{E52}$$

into corners of a skeleton diagram yield no additional divergences.

For reducible vertex diagrams, the V-part resolves into a skeleton along with stabilized SE- and V-part insertions. With replacements (E50), (E51), and (E52) in the skeleton, the vertex operator again reduces to the form (E40), where $L \rightarrow L_s$ is the skeleton divergence. In general, L_s depends on multiple functions $D_{\circ}$ corresponding to all possible

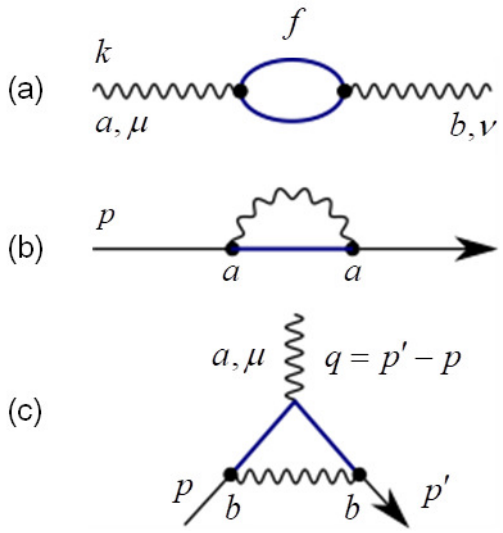

Figure 5. Gluon/quark self-energies and vertex diagrams

charged fermion masses arising from photon self-energy insertions which may in turn contain SE- and V-parts. Since each $D_\circ$ is invariant under equation (D6), (E46) holds, and (21) yields

$$\overline{\Lambda}_s^\mu = \gamma^\mu L_s \tag{E53}$$

similarly to equation (E43); therefore, the complete reducible V-part given by equation (E49) is convergent.

For reducible self-energy diagrams, a skeleton with SE insertions is handled in the same way as reducible vertex diagrams. However, vertex insertions into fermion and photon SE skeletons involve overlapping divergences that require further analysis [52, 79]. Integration of Ward's identities yields expressions of the same form as equations (E38) and (E39); in this case, the coefficients $\{A, B, C\}$ are all power series in α depending on $D_\circ$, and vertex insertions in SE-parts are convergent upon including stability corrections (E41) and (E42). We conclude that infinite field actions excite dressed mass levels uniformly in all connected fermion lines internal to overlapping loops; for a specific example, apply (20) to calculate the real part of the fourth-order vacuum polarization kernel [80] using the dispersion method given in Appendix E 1. Therefore, a diagram with overlapping divergences is not a special case for implementation of stability corrections.

The complete propagators, replacing fermion and photon lines in a skeleton diagram, follow from equations (63) and (64) of [6]; one obtains

$$S'_F(p) = \frac{i}{\not{p} - m - \hat{\Sigma}^* + i\varepsilon}, \tag{E54}$$

$$D'^{\alpha\beta}_F(k) = \frac{-ig^{\alpha\beta}}{k^2\left[1 - \hat{\Pi}^*\right] + i\varepsilon}, \tag{E55}$$

where $\left\{\hat{\Sigma}^*, \hat{\Pi}^*\right\}$ are given by sums over all proper SE-parts. Similarly, the most general vertex replacing a corner in a skeleton diagram is given by a sum over all proper V-parts. Since both core and stability corrections are included in each sub-diagram, the complete propagators and vertices are well defined (convergent).

Appendix F: QCD verification

In the examples below, we focus on a key subset of one-loop diagrams [49, 53] that occur in the $SU(3)$ Yang-Mills theory; see Appendix C 2 for nomenclature.

For diagrams in Fig. 5, core amplitudes differ from QED only by group factors and switching factor λ_s from (32);

therefore, finite S-matrix amplitudes (31), including stability corrections, are

$$\hat{\Pi}_1^{ab} = \lambda_s \mathrm{tr}\left(t^a t^b\right) \hat{\Pi}\left[QED\right] , \tag{F1}$$

$$\hat{\Sigma}^{aa} = \lambda_s t^a t^a \hat{\Sigma}\left[QED\right] , \text{ and} \tag{F2}$$

$$\hat{\Lambda}_1^{a,\mu} = \lambda_s t^b t^a t^b \hat{\Lambda}^\mu\left[QED\right] . \tag{F3}$$

Group factors are given by

$$\begin{aligned} \mathrm{tr}\left(t^a t^b\right) &= C\left(r\right)\delta^{ab} , \\ t^a t^a &= C_2\left(r\right) , \\ t^b t^a t^b &= \left[C_2\left(r\right) - \frac{1}{2}C_2\left(G\right)\right] t^a , \end{aligned}$$

where $C(N) = \frac{1}{2}$ and $C_2\left(N\right) = \frac{N^2-1}{2N} = \frac{4}{3}$ are normalization and quark color charge factors, respectively.

In addition to the fermion (quark) loop diagram in Fig. 5 (a), gluon self-energy corrections in Fig. 6 yield [51]

$$\left[\text{Fig. 6}\right] = iT_{\mu\nu}\left(k^2\right)\delta^{ab}\Pi_2\left(k^2\right) , \tag{F4}$$

$$T_{\mu\nu}\left(k^2\right) = g_{\mu\nu}k^2 - k_\mu k_\nu ,$$

$$\Pi_2\left(k^2\right) = \frac{\alpha_s C_2\left(G\right)}{4\pi}\int_0^1 dx\, \frac{\Gamma\left(\sigma\right)}{\Delta^\sigma}\left[\left(\sigma-1\right)\left(1-2x\right)^2 + 2\right] , \tag{F5}$$

where $\alpha_s = g_s^2/4\pi$ is the strong coupling constant, $\Delta = -k^2 x\left(1-x\right)$, and x is a Feynman parameter. While individual gluons are massless to ensure gauge invariance of $\mathcal{L}_{YM}$, systems of gluons depicted in Fig. 6 are expected to have a non-zero mass defined by (8) with self-energy function

$$\Sigma^g \sim k^2\Pi_2 . \tag{F6}$$

The generation of such systems redistributes vacuum energy as indicated in Fig. 2. Consequently, we need to include a stability correction involving DCM states, but for this we need a mass term in Δ. If we appeal to massive Yang-Mills theories [81], we get unwanted particles and ghosts, and it might seem that we have an impasse. While gauge invariance demands that mass be acquired via a Higgs mechanism, introduction of dressed masses in (C29) yielding

$$\mathcal{L}'_{YM} \to \mathcal{L}_{YM} - \frac{1}{2}\sum_{\lambda=\pm1}\left[\mu_g^2 + \lambda M_g^2\right]_{\mu_g=0}\left(A_\mu^a\right)^2 \tag{F7}$$

does not break gauge invariance of $\mathcal{L}_{YM}$ since its sum is zero. Therefore, let us temporarily assign a small mass μ_g to the gluon, then propagators in the loops are modified

$$\frac{1}{p^2-\mu_g^2}\frac{1}{\left(p+k\right)^2-\mu_g^2} = \int_0^1 \frac{dx}{\left[P^2 - \Delta\left(\mu_g\right)\right]^2} , \tag{F8}$$

where the usual change of variables $P = p + xk$ has been made for loop integration parameter p, and

$$\Delta\left(\mu_g\right) = \mu_g^2 - k^2 x\left(1-x\right) .$$

To evaluate the stability contribution, let $M_g = \eta\mu_\circ$, where $\mu_\circ$ is an arbitrary unit of mass measure. Substituting

$$\mu_g^2 \to \left[\mu_g^2 + \lambda\eta^2\mu_\circ^2\right]_{\mu_g=0} \tag{F9}$$

in $\Delta\left(\mu_g\right)$ and using equation (D12), we have $\Delta_\circ = \mu_\circ^2$. Negating equation (F5), replacing

$$\frac{1}{\Delta^\sigma} \to \frac{1}{\Delta_\circ^\sigma} ,$$

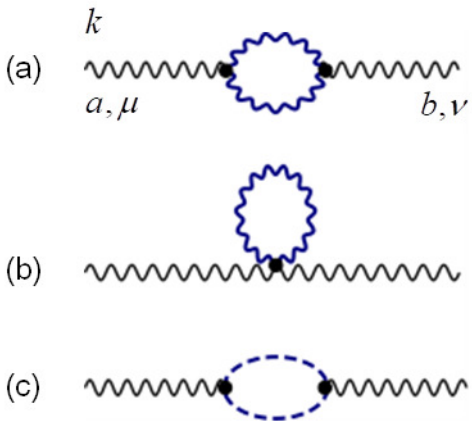

Figure 6. Gluon self-energy corrections in pure-gauge sector: (a) gluon loop, (b) four-gluon vertex, and (c) ghost loop.

and using (31), the net amplitude

$$\hat{\Pi}_2\left(k^2\right) = -\lambda_s \frac{\alpha_s C_2\left(G\right)}{4\pi} \int_0^1 dx\, \ln\left[\frac{-k^2 x\left(1-x\right)}{\mu_\circ^2}\right]\left[2-\left(1-2x\right)^2\right] \tag{F10}$$

is finite. If we define a reference mass M_s by

$$\frac{5}{3}\ln\left(\frac{\mu_\circ^2}{M_s^2}\right) \equiv \int_0^1 dx\, \ln\left[x\left(1-x\right)\right]\left[2-\left(1-2x\right)^2\right] ,$$

then

$$\hat{\Pi}_2\left(\rho_s \equiv -\frac{k^2}{M_s^2}\right) = -\lambda_s \frac{\alpha_s C_2\left(G\right)}{4\pi}\frac{5}{3}\ln\rho_s \tag{F11}$$

vanishes at spacelike $k^2 = -M_s^2$. For physically meaningful interpretation of the amplitudes, unobservable quark and gluon states must have negative norm and spacelike momenta.

In the stabilized theory, it is invalid to neglect quark masses m_f in the calculations since they are required for defining dressed amplitudes, but QCD calculations in the usual theory often omit m_f in processes where the momentum transfer q is presumed much larger than physical masses involved in the problem. Therefore, following [51], but assuming $m \equiv m_f \neq 0$, the stabilized integral for the quark/three-gluon vertex shown in Fig. 7 is

$$\hat{\Lambda}_2^{a,\mu} = i\lambda_s \frac{g_s^2 C_2\left(G\right) t^a}{\left(2\pi\right)^4} \int dxdydz\, \delta\left(x+y+z-1\right) \Delta I^\mu ,$$

where (x, y, z) are Feynman parameters; keeping only leading logarithmic terms,

$$\begin{aligned} \Delta I^\mu &\simeq I^\mu - \overline{I}^{\,\mu} \\ &= 3i\pi^2\gamma^\mu \ln\frac{\Delta}{\Delta_\circ} , \end{aligned}$$

$$I^\mu = -3i\pi^2\gamma^\mu \frac{\Gamma\left(\sigma\right)}{\Delta^\sigma} ,$$

$$\Delta = m^2 z + \left(px + p'y\right)^2 - p^2 x - p'^2 y + \mu^2\left(1-z\right) ,$$

$$\overline{I}^{\,\mu} = -3i\pi^2\gamma^\mu \frac{\Gamma\left(\sigma\right)}{\Delta_\circ^\sigma} ,$$

and

$$\Delta_\circ = m^2 z^2 + \mu^2 (1 - z)$$

follows from equation (D4). Assuming p is on mass shell and $-q^2 \gg m^2 \gg \mu^2$, $\Delta \simeq -q^2 y (1 - y)$ and $\Delta_\circ \simeq m^2 z^2$; therefore,

$$\Delta I^\mu \simeq 3i\pi^2 \gamma^\mu \ln \frac{-q^2}{m^2} + \text{ H.O.T. } .$$

Higher order terms in ΔI^μ integrate to $O(1)$ in (F12), and we have

$$\hat{\Lambda}_2^{a,\mu} = -\lambda_s \frac{\alpha_s}{4\pi} \frac{3}{2} C_2 (G)\, t^a \gamma^\mu \ln \frac{-q^2}{m^2} \, . \tag{F13}$$

It remains to show that the stabilized theory agrees with standard renormalization theory and experimental data [66] ; in particular, an effective weakening of the strong coupling for high energies consistent with asymptotic freedom predictions [20, 21]. Well known formulae from SRT are used, where renormalization constants are replaced with stabilized amplitude parameters

$$Z_i \to \hat{Z}_i \, , \; i = 1, 2, 3 \, .$$

Leading terms of stabilized amplitudes for the asymptotic case of high energy yield an effective color charge

$$\begin{aligned} \overline{g}_s (\rho_s) &= g_s \frac{\hat{Z}_1}{\hat{Z}_2 \sqrt{\hat{Z}_3}} \\ &\simeq g_s \left[1 + \lambda_s \frac{\alpha_s}{8\pi} \left(11 - \frac{2}{3} n_f \right) \ln \rho_s \right] \, , \end{aligned} \tag{F14}$$

where

$$\hat{Z}_1^{-1} = 1 + \hat{\Lambda}_1 (\rho_s) + \hat{\Lambda}_2 (\rho_s) \, , \tag{F15}$$

$$\hat{Z}_2^{-1} = 1 - \left. \frac{d\hat{\Sigma}}{d\not{p}} \right|_{\rho = \rho_s} \, , \text{ and} \tag{F16}$$

$$\hat{Z}_3^{-1} = 1 - \left[\hat{\Pi}_1 (\rho_s) + \hat{\Pi}_2 (\rho_s) \right] \tag{F17}$$

are finite running stabilization parameters that modify the vertex (C30), fermion field propagator (C25), and gluon field propagator (C33), respectively. For loops including quarks, asymptotic amplitudes involve spacelike momenta ℓ in quadratic energy ratios

$$\rho = -\frac{\ell^2}{m_f^2} \gg 1 \, ; \; \ell^2 \in \left\{ k^2, \, p^2, \, q^2 \right\} \, , \tag{F18}$$

where we have reinstated $m_f = m$. Setting $p^2 = q^2 = k^2$ across diagrams and neglecting $O(1)$ terms in

$$\begin{aligned} \ln \rho &= \ln \rho_s + O(1) \\ &\simeq \ln \rho_s \, , \end{aligned} \tag{F19}$$

where $\rho_s = -k^2 / M_s^2$, the sum over fermions in Fig. 5 (a) becomes trivial, and we have

$$\sum_{f=1}^{n_f} \left\{ [\text{Fig. 5(a)}] = \underset{a,\mu}{\overset{k}{\sim}} \overset{f}{\bigcirc} \underset{b,\nu}{\sim} \right\} \simeq i T_{\mu\nu} \left(k^2 \right) \delta^{ab} \left[\hat{\Pi}_1 (\rho_s) \equiv \lambda_s \frac{\alpha_s}{3\pi} n_f \, C(r) \ln \rho_s \right] \, , \tag{F20}$$

$$[\text{Fig. 5(b)}] \simeq -i \left[\hat{\Sigma} (\not{p}, \rho_s) \equiv \lambda_s \frac{\alpha_s}{4\pi} C_2 (r) (\not{p} - 4 m_f) \ln \rho_s \right] \, , \tag{F21}$$

$$[\text{Fig. 5(c)}] \simeq i g_s t^a \gamma^\mu \left\{ \hat{\Lambda}_1 (\rho_s) \equiv -\lambda_s \frac{\alpha_s}{4\pi} \left[C_2 (r) - \frac{1}{2} C_2 (G) \right] \ln \rho_s \right\} \, , \tag{F22}$$

$$[\text{Fig. 6}] = i T_{\mu\nu} \left(k^2 \right) \delta^{ab} \left[\hat{\Pi}_2 (\rho_s) \equiv -\lambda_s \frac{\alpha_s}{4\pi} C_2 (G) \frac{5}{3} \ln \rho_s \right] \, , \text{ and} \tag{F23}$$

$$[\text{Fig. 7}] \simeq i g_s t^a \gamma^\mu \left[\hat{\Lambda}_2 (\rho_s) \equiv -\lambda_s \frac{\alpha_s}{4\pi} C_2 (G) \frac{3}{2} \ln \rho_s \right] \, . \tag{F24}$$

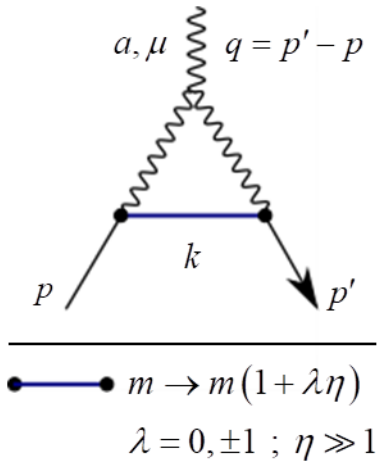

Figure 7. Quark/three-gluon vertex.

With the approximation $-k^2 \gg m_f^2$, $\hat{\Pi}_1$ in equation (F20) follows from (F1) using (E7). Similarly, $\hat{\Sigma}$ in equation (F21) is obtained from (F2) using (E19), and $\hat{\Lambda}_1$ in equation (F22) is derived using (F3) with (E36). The stabilization parameters $\hat{Z}_1$, $\hat{Z}_2$, and $\hat{Z}_3$ are defined similarly to their SRT counterparts. $\hat{Z}_1^{-1}$ is the coefficient of $ig_s\gamma^\mu t^a$ for the sum of proper vertex diagrams in equation (C30), Fig. 5 (c), and Fig. 7:

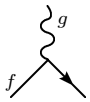

$$\cdot \left(1 + \hat{\Lambda}_1 + \hat{\Lambda}_2\right) \equiv ig_s\gamma^\mu t^a \hat{Z}_1^{-1} \,. \tag{F25}$$

Using equation (E26) or (F16) and assuming $-p^2 \gg m_f^2$, we have

$$\hat{Z}_2^{-1} = 1 - \lambda_s \frac{\alpha_s}{4\pi} C_2(r) \left[\ln\rho = \ln\rho_s + O(1)\right] \,. \tag{F26}$$

For $\hat{Z}_3$, equation (E9) is used with $\hat{\Pi} = \hat{\Pi}_1 + \hat{\Pi}_2$, (F20), and (F23).

Finally, using (F14), the effective coupling constant is reduces to

$$\overline{\alpha}_s(\rho_s) = \frac{\alpha_s}{1 - \lambda_s \frac{\alpha_s}{4\pi}\left(11 - \frac{2}{3}n_f\right)\ln\rho_s + O\left(\ln^2\rho_s\right)} \,. \tag{F27}$$

Neglecting terms of $O\left(\ln^2\rho_s\right)$ for ρ_s near one and requiring $\lambda_s = -1$, (F27) reduces to the expected result for asymptotic freedom. The corresponding [47, 48] beta function is

$$\beta_{QCD} = 2\frac{\partial\,\overline{\alpha}_s}{\partial \ln\rho_s}\bigg|_{\rho_s=1} = \lambda_s \frac{\alpha_s^2}{2\pi}\left(11 - \frac{2}{3}n_f\right) \,. \tag{F28}$$

The foregoing results are consistent with Fig. 2 and in complete agreement with standard QFT. The effective color charge in equation (F14) is defined relative to a stable value g_s defined at $\rho_s = 1$, where the gluon polarization function (F11) vanishes; for $\rho_s > 1$, $\hat{\Pi}_2(\rho_s)$ goes positive. In contrast, low energy electron scattering processes probe the far-field (positive energy) region, and a stable value for the electric charge is defined in the free particle limit: $k^2 = 0$, where the polarization function $\hat{\Pi}\left(k^2\right)$ vanishes; refer to equations (E7)-(E11).

An estimate of M_s may be obtained by synchronizing ρ in equation (F18) across diagrams in Fig. 5 (a) with that for ρ_s in equation (F11) for Fig. 6: Let $k \to \ell$ in Fig. 5 (a), and require

$$\frac{\ell^2}{m_f^2} = \frac{k^2}{M_s^2} \,. \tag{F29}$$

Noting that $\hat{\Pi}[QED]$ is a function of ρ only from equation (E7) and using (F29), the sum over fermions is given by

$$\sum_{f=1}^{n_f} \quad \underset{a,\mu}{\overset{\ell}{\sim}}\!\!\bigcirc^{f}\!\!\sim_{b,\nu} = \left[\left(\frac{1}{n_f}\sum_{f=1}^{n_f}\frac{m_f^2}{M_s^2}\right) \equiv 1\right] n_f \quad \underset{a,\mu}{\overset{k}{\sim}}\!\!\bigcirc^{f}\!\!\sim_{b,\nu} \,. \tag{F30}$$

The condition in brackets is obtained by factoring

$$T_{\mu\nu}\left(\ell^2\right) = \frac{m_f^2}{M_s^2} T_{\mu\nu}\left(k^2\right)$$

and comparing with (F20), then we have

$$M_s^2 = \frac{1}{n_f}\sum_{f=1}^{n_f} m_f^2 \tag{F31}$$

for the reference mass. Evaluating (F31) for quarks gives $M_s = 70.65\, GeV/c^2$; compare with Z–boson mass given in Appendix G 6: Table II.

Appendix G: Electroweak verification

We compute finite electroweak amplitudes using dimensionally regularized radiative corrections for unrenormalized (core) functions [43, 67, 82]. One-loop self-energy functions include Σ^{ab} for bosons, where

$$ab \in \{\gamma\gamma,\, \gamma Z,\, ZZ,\, WW\}$$

defines particles external to the loop, Σ^f for fermions ($f = j\sigma$ for doublet j and component $\sigma = \pm$), and vertex $\Lambda_\mu^{\gamma f}$. For repeated indices $a = b$, we abbreviate $\Sigma^b \equiv \Sigma^{bb}$ with $b \in \{\gamma,\, Z,\, W\}$; in general formulae applicable to $\gamma - Z$ mixing, we admit $b = \gamma Z$ as well for brevity. A subscript "sa" is appended to a stabilized amplitude $\hat{\Sigma}^b \equiv \hat{\Sigma}^b_{sa}$ when it is necessary to distinguish it from a corresponding renormalized amplitude $\hat{\Sigma}^b_{ra}$.

In Hollik's notation [43], the basic singular function

$$\Delta_\kappa = \frac{1}{\sigma} - \gamma - \ln\frac{m_\kappa^2}{\mu^2} + \ln 4\pi\,, \tag{G1}$$

involving a mass scale μ, differs from (D7) by finite terms. For consistency, the input momentum to a loop is k with $s \equiv k^2$ for both bosons and fermions. Abbreviations for squared boson masses

$$z = m_Z^2\,, \quad w = m_W^2\,, \text{ and } \quad h = m_H^2$$

are used. In addition to (G1), core amplitudes involve finite functions

$$\overline{B}_\circ\left(s, m_1, m_2\right) = -\int_0^1 dx\, \ln\left[\frac{x^2 s - x\left(s + m_1^2 - m_2^2\right) + m_1^2 - i\epsilon}{m_1 m_2}\right]\,, \tag{G2}$$

$$F\left(s, m_1, m_2\right) = -1 + \frac{m_1^2 + m_2^2}{m_1^2 - m_2^2}\ln\frac{m_1}{m_2} + \overline{B}_\circ\left(s, m_1, m_2\right)\,, \tag{G3}$$

$$\overline{B}_1\left(s, m_1, m_2\right) = -\frac{1}{4} + \frac{m_1^2}{m_1^2 - m_2^2}\ln\frac{m_1}{m_2} + \frac{m_2^2 - m_1^2 - s}{2s}F\left(s, m_1, m_2\right)\,, \tag{G4}$$

and singular expressions

$$B_\circ\left(s, m_1, m_2\right) = \frac{1}{2}\left(\Delta_{m_1} + \Delta_{m_2}\right) + \overline{B}_\circ\left(s, m_1, m_2\right)\,, \tag{G5}$$

$$B_1\left(s, m_1, m_2\right) = -\frac{1}{2}\left(\Delta_{m_2} + \frac{1}{2}\right) + \overline{B}_1\left(s, m_1, m_2\right)\,. \tag{G6}$$

Scalar one-loop integrals, including (G2), are defined in [83].

1. Boson self-energy corrections

For these corrections, it is useful to expand the boson self-energy

$$\Sigma^b(s) = \Sigma^b\left(m_b^2\right) + \sum_{n=1}^{\infty} \left.\frac{\partial^n \Sigma^b}{\partial s^n}\right|_{s=m_b^2} \left(s - m_b^2\right)^n \ . \tag{G7}$$

From core amplitudes, it can be seen by inspection and dimensional analysis that averages of $\Sigma^b\left(m_b^2\right)$ and $\left.\frac{\partial \Sigma^b}{\partial s}\right|_{s=m_b^2}$ over DCM levels in equation (21) are stationary. For mass set

$$\{m_\kappa\} \subseteq \{m_f,\, m_W,\, m_Z,\, m_H\} \ ,$$

the DCM transform (12) is

$$\left\{m_\kappa^2\right\} \to \left\{m_\kappa^2\right\} \cdot \left(1 + \lambda\eta^2\right) \ . \tag{G8}$$

On the mass shell, the self-energy function has the general form

$$\Sigma^b\left(m_b^2\right) = \sum_\kappa \alpha_\kappa^b m_\kappa^2 \, , \tag{G9}$$

where α_κ^b are dimensionless coefficients which may depend on invariant mass ratios. Therefore, under (G8)

$$\Sigma^b\left(m_b^2\right) \to \left(1 + \lambda\eta^2\right) \Sigma^b\left(m_b^2\right) \ , \tag{G10}$$

and the average

$$\begin{aligned} \overline{\Sigma}^b\left(m_b^2\right) &= \frac{1}{2} \sum_{\lambda=\pm 1} \left(1 + \lambda\eta^2\right) \Sigma^b\left(m_b^2\right) \\ &= \Sigma^b\left(m_b^2\right) \end{aligned} \tag{G11}$$

over dressed states is stationary. Since the derivative $\left.\frac{\partial \Sigma^b}{\partial s}\right|_{s=m_b^2}$ is dimensionless, it is invariant under (G8). Finally, higher order derivatives are either zero outright, or

$$\left.\frac{\partial^n \Sigma^b}{\partial s^n}\right|_{s=m_b^2} \sim \left(m_b^2\right)^{1-n} \to O\left(\eta^{2(1-n)}\right) \tag{G12}$$

vanishes under (G8) as $\eta \to \infty$ for $n \geq 2$. Therefore, we have

$$\overline{\Sigma}^b(s) = \Sigma^b\left(m_b^2\right) + \left.\frac{\partial \Sigma^b}{\partial s}\right|_{s=m_b^2} \left(s - m_b^2\right) \ . \tag{G13}$$

Since the off-shell factor $s - m_b^2 = \delta k_{os}^2$ is stationary from (17), the entire expression (G13) is stationary under an average over DCM levels similarly to (G11). The net stabilized amplitude

$$\hat{\Sigma}^b(s) = \Sigma^b(s) - \overline{\Sigma}^b(s) \tag{G14}$$

satisfies stability conditions

$$\hat{\Sigma}^b\left(m_b^2\right) \ = \ 0 \, , \tag{G15}$$

$$\left.\frac{\partial \hat{\Sigma}^b(s)}{\partial s}\right|_{s=m_b^2} \ = \ 0 \, . \tag{G16}$$

Taking the real part of (G15) and (G16) yields renormalization conditions [50], which differ from those given in [43]. For stabilized amplitude (G14), (G15) and (G16) yield a propagator residue of unity so there is no need for external wave function corrections as in the on-shell renormalization scheme proposed by [84]; however, inclusion of

Δr corrections [42] discussed in Appendix G 4 leads to finite wave field corrections. Splitting off singular terms (G1), the boson self-energy can be expressed in the form

$$\Sigma^b(s) = \sum_\kappa \left[\alpha^b_\kappa s\Delta_\kappa + \beta^b_\kappa m^2_\kappa \Delta_\kappa\right] + \Sigma^b_{finite}(s) \ , \tag{G17}$$

where $\left\{\alpha^b_\kappa, \beta^b_\kappa\right\}$ are constant coefficients. Singular terms involving $\left\{s\Delta_\kappa,\, m^2_\kappa\Delta_\kappa\right\}$ in $\overline{\Sigma}^b$ cancel those in Σ^b, and (G14) reduces to

$$\hat{\Sigma}^b(s) = \Sigma^b_{finite}(s) - \Sigma^b_{finite}\left(m^2_b\right) - \left.\frac{\partial \Sigma^b_{finite}}{\partial s}\right|_{s=m^2_b}\left(s - m^2_b\right) \ . \tag{G18}$$

For a free boson, the squared mass shift

$$\delta m^2_b \equiv \mathrm{Re}\left[\Sigma^b_{finite}\left(m^2_b\right)\right] \tag{G19}$$

represents the residual boson self-energy of the core amplitude after divergent parts of $\overline{\Sigma}^b\left(m^2_b\right)$ have canceled those in (G17). For later reference, the polarization function is

$$\hat{\Pi}^b(s) = \frac{\hat{\Sigma}^b(s)}{s - m^2_b} = \frac{\Sigma^b(s) - \Sigma^b\left(m^2_b\right)}{s - m^2_b} - \left.\frac{\partial \Sigma^b}{\partial s}\right|_{s=m^2_b} \ . \tag{G20}$$

Neglecting Δr corrections, mixing angle functions $c_w = \cos\theta_W$ and $s_w = \sin\theta_W$ from equation (C10), and neutral current constants (C24) are invariant under equation (G8). See equations (G30) and (G31) for inclusion of Δr.

Application of (G14) to photon self-energy corrections shown in Fig. 8 yields

$$\begin{aligned}
\hat{\Sigma}^\gamma(s) &= \Sigma^\gamma(s) - \overline{\Sigma}^\gamma(s) \\
&= \frac{\alpha}{4\pi}\left\{\frac{4}{3}\sum_f Q^2_f\left[\left(s + 2m^2_f\right)F\left(s, m_f, m_f\right) - \frac{s}{3}\right]\right. \\
&\quad \left. - (3s + 4w)\,F(s, m_W, m_W) + \frac{2}{3}s\right\} \ ,
\end{aligned} \tag{G21}$$

$$\begin{aligned}
\Sigma^\gamma(s) &= \frac{\alpha}{4\pi}\left\{\frac{4}{3}\sum_f Q^2_f\left[s\Delta_f + \left(s + 2m^2_f\right)F\left(s, m_f, m_f\right) - \frac{s}{3}\right]\right. \\
&\quad \left. - 3s\Delta_W - (3s + 4w)\,F(s, m_W, m_W)\right\} \ ,
\end{aligned} \tag{G22}$$

$$\overline{\Sigma}^\gamma(s) = \Sigma^\gamma(0) + \left.\frac{\partial \Sigma^\gamma}{\partial s}\right|_{s=0} s \ , \tag{G23}$$

where

$$\begin{aligned}
\Sigma^\gamma(0) &= 0 \ , \\
\left.\frac{\partial \Sigma^\gamma}{\partial s}\right|_{s=0} &= \frac{\alpha}{4\pi}\left\{\frac{4}{3}\sum_f Q^2_f\Delta_f - 3\Delta_W - \frac{2}{3}\right\} \ ,
\end{aligned}$$

and the sum over fermions includes color for the case of quarks. Both $\hat{\Sigma}^\gamma(s)$ and $\hat{\Pi}^\gamma(s)$ vanish in the Thomson limit $s \to 0$, and physically meaningful corrections in equation (G21) are due to incomplete cancellation for $s = k^2 \neq 0$. Singular terms in $\overline{\Sigma}^\gamma$ exactly cancel those in Σ^γ for all s, and there remains a term

$$\left[\overline{\Sigma}^\gamma\right]_{finite} = -\left(\delta\alpha_{finite} \equiv \frac{\alpha}{6\pi}\right)s \tag{G24}$$

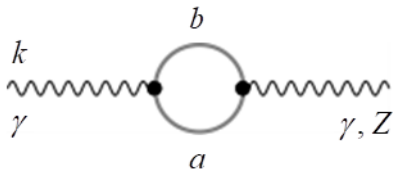

a	b
$\bar{f}$	f
W	W
ϕ	W
ϕ	ϕ
$u^{\pm}$	$u^{\mp}$
†	W, ϕ

† Four gauge boson vertex with internal W,ϕ

Figure 8. Photon self-energy and photon-Z mixing diagrams.

in the vacuum response, where $\delta\alpha_{finite}$ is the finite part of renormalization constant δZ_2^{γ} in the usual theory.

For $\gamma - Z$ mixing corrections also represented in Fig. 8, we have

$$\begin{aligned}\hat{\Sigma}^{\gamma Z}(s) &= \Sigma^{\gamma Z} - \overline{\Sigma}^{\gamma Z} \\ &= \frac{\alpha}{4\pi}\left\{-\frac{4}{3}\sum_f Q_f v_f\left[\left(s+2m_f^2\right)F\left(s,m_f,m_f\right)-\frac{s}{3}\right]\right. \\ &\quad \left.+\frac{1}{c_w s_w}\left[\left(3c_w^2+\frac{1}{6}\right)s+\left(4c_w^2+\frac{4}{3}\right)w\right]F\left(s,m_W,m_W\right)-\frac{s}{6c_w s_w}\left(4c_w^2+\frac{4}{3}\right)\right\},\end{aligned} \tag{G25}$$

$$\begin{aligned}\Sigma^{\gamma Z}(s) &= \frac{\alpha}{4\pi}\left\{-\frac{4}{3}\sum_f Q_f v_f\left[s\Delta_f+\left(s+2m_f^2\right)F\left(s,m_f,m_f\right)-\frac{s}{3}\right]\right. \\ &\quad +\frac{1}{c_w s_w}\left[\left(3c_w^2+\frac{1}{6}\right)s+2w\right]\Delta_W \\ &\quad \left.+\frac{1}{c_w s_w}\left[\left(3c_w^2+\frac{1}{6}\right)s+\left(4c_w^2+\frac{4}{3}\right)w\right]F\left(s,m_W,m_W\right)+\frac{s}{9c_w s_w}\right\},\end{aligned} \tag{G26}$$

$$\overline{\Sigma}^{\gamma Z} = \Sigma^{\gamma Z}(0) + \left.\frac{\partial\Sigma^{\gamma Z}}{\partial s}\right|_{s=0} s\,, \tag{G27}$$

where

$$\begin{aligned}\Sigma^{\gamma Z}(0) &= \frac{\alpha}{4\pi}\left\{\frac{2w}{c_w s_w}\Delta_W\right\}, \\ \left.\frac{\partial\Sigma^{\gamma Z}}{\partial s}\right|_{s=0} &= \frac{\alpha}{4\pi}\left\{-\frac{4}{3}\sum_f Q_f v_f\Delta_f+\frac{1}{c_w s_w}\left[\left(3c_w^2+\frac{1}{6}\right)\Delta_W+\frac{1}{6}\left(4c_w^2+\frac{4}{3}\right)+\frac{1}{9}\right]\right\},\end{aligned}$$

and $\Sigma^{\gamma Z}(0) \neq 0$ is due to non-Abelian boson loops in Fig. 8.

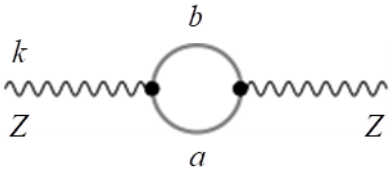

a	b
$\bar{f}$	f
W	W
ϕ	W
H	Z
χ	H
ϕ	ϕ
$u^{\pm}$	$u^{\mp}$
†	W, H, χ, ϕ

Figure 9. Z-boson self-energy.

Renormalization starts with a bare charge $e_\circ$, and the correction [67]

$$\begin{aligned} \delta e\left(\Pi^{\gamma}, \Sigma^{\gamma Z}\right) &= e_\circ\left[\delta Z_1^{\gamma} - \frac{3}{2}\delta Z_2^{\gamma}\right] \\ &= e_\circ\left[\frac{1}{2}\Pi^{\gamma}(0) - \frac{s_w}{c_w}\frac{\Sigma^{\gamma Z}(0)}{m_Z^2}\right] \end{aligned} \tag{G28}$$

renormalizes the charge $e = e_\circ + \delta e$, where

$$\begin{aligned} \delta Z_1^{\gamma} &= -\Pi^{\gamma}(0) - \frac{s_w}{c_w}\frac{\Sigma^{\gamma Z}(0)}{m_Z^2}\,, \\ \delta Z_2^{\gamma} &= -\Pi^{\gamma}(0) \end{aligned}$$

are the charge and photon field renormalization constants, respectively. In the usual theory, arguments on the left in equation (G28) are core functions $\left\{\Pi^{\gamma},\, \Sigma^{\gamma Z}\right\}$; however, in the stabilized theory, we utilize the complete amplitudes (G21) and (G25) to obtain

$$\delta e\left(\hat{\Pi}^{\gamma}, \hat{\Sigma}^{\gamma Z}\right) = 0\,. \tag{G29}$$

Therefore, $e = e_\circ$, and there is no charge renormalization.

Self-energy diagrams for the $Z-$ and $W-$bosons are tabulated in Figs. 9 and 10, respectively. Due to their complexity, analytic expressions for the unrenormalized amplitudes [43] are omitted here, but the stabilized amplitudes are easily evaluated using (G13) and analytic expressions for partials $\frac{\partial \Sigma^b}{\partial s}$. Plots of these functions are given in Appendix G 6.

Self-energies for diagrams with $b \in \{\gamma Z,\, Z,\, W\}$ require adjustments

$$\hat{\Sigma}^b(s) \to \hat{\Sigma}^b(s) + \left(s - m_b^2\right)\Delta r^b \quad (b = W, Z)\,, \tag{G30}$$

$$\hat{\Sigma}^{\gamma Z}(s) \to \hat{\Sigma}^{\gamma Z}(s) + s\Delta r^{\gamma Z} \tag{G31}$$

for Δr corrections [42] which account for variations of $\{g_W, g_Z\}$ with respect to m_W and m_Z; we have

$$\left\{\Delta r^{\gamma Z},\, \Delta r^{Z},\, \Delta r^{W}\right\} = \left\{-\frac{c_w}{s_w},\, \frac{c_w^2 - s_w^2}{s_w^2},\, \frac{c_w^2}{s_w^2}\right\}\left(\frac{\delta m_Z^2}{m_Z^2} - \frac{\delta m_W^2}{m_W^2}\right)\,, \tag{G32}$$

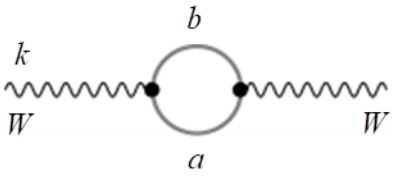

a	b
f^-	f^+
W	Z
ϕ	Z
W	γ
ϕ	γ
H	W
ϕ	H
ϕ	χ
u^Z	$u^\pm$
u^γ	$u^\pm$
†	Z, W, H, χ, ϕ

Figure 10. W-boson self-energy.

wherein finite-on-shell-mass shifts from (G19) are

$$\delta m_Z^2 = \mathrm{Re}\left[\Sigma_{finite}^Z\left(m_Z^2\right)\right] , \tag{G33}$$

$$\delta m_W^2 = \mathrm{Re}\left[\Sigma_{finite}^W\left(m_W^2\right)\right] . \tag{G34}$$

In Appendix G 4, we derive Δr^b using stability arguments. Values for squared mass ratios

$$\left\{\frac{\delta m_Z^2}{m_Z^2}, \frac{\delta m_W^2}{m_W^2}\right\}$$

and Δr are given in Table II in Appendix G 6.

Net amplitudes for boson self-energies are finite and satisfy required mass shell conditions (G15) and (G16) for $b \in \{\gamma, \gamma Z, Z, W\}$. Amplitude $\hat{\Sigma}^\gamma$ agrees with the result given in [43]; however,

$$\left\{\hat{\Sigma}^{\gamma Z}, \hat{\Sigma}^Z, \hat{\Sigma}^W\right\}$$

including Δr corrections, differ from Hollik's results in two respects:

a) A small finite charge renormalization $\frac{\alpha}{6\pi} = 3.87 \times 10^{-4}$ from (G24) is absent in $\left\{\hat{\Sigma}^Z, \hat{\Sigma}^W\right\}$, and

b) they include polarization derivative shifts in (G20) — finite parts are given in Appendix G 6: Table II.

As regards item a), inclusion of any charge renormalization would be inconsistent with the stability approach and result (G29) in particular. For item b), finite parts differ depending on the renormalization scheme, and $\left\{\hat{\Sigma}^{\gamma Z}, \hat{\Sigma}^Z, \hat{\Sigma}^W\right\}$ are consistent with the scheme given in [50]; moreover, all four boson self-energies are unified under the same formula (G14). Numerical results for boson polarization functions are given in Appendix G 6.

2. Fermion self-energy corrections

For fermion self-energy corrections, we again expand the core amplitude

$$\Sigma^f(k) = \Sigma^f(m_f) + \left.\frac{\partial \Sigma^f}{\partial \not{k}}\right|_{\not{k}=m_f} (\not{k} - m_f) + H.O.T.\,. \tag{G35}$$

From (11), the DCM transform is

$$\{m_\kappa\} \to \{m_\kappa\} \cdot (1 + \lambda\eta)\ , \tag{G36}$$

where the mass set $\{m_\kappa\} \subseteq \{m_f,\, m_W,\, m_Z,\, \mu\}$ corresponds to terms in (G41). Upon applying equation (21) to (G35) and noting that $\left\{B_i\left(m_f^2, m_1, m_2\right);\, i = 0, 1\right\}$ occurring in equation (G41) are invariant under (G36) applied to all mass arguments, we obtain

$$\left.\overline{\Sigma}^f(k)\right|_{\not{k}=m_f} = \Sigma^f(m_f)\ . \tag{G37}$$

From arguments similar to those for boson self-energies above, $\not{k} - m_f$ is stationary from equation (16), and its dimensionless coefficient (first partial) in (G35) is invariant under (G36). The first partial involves derivatives of $B_\circ$ and B_1 in equations (G5) and (G6), respectively. Finally, higher-order terms in equation (G35) vanish under (G36), and we have

$$\overline{\Sigma}^f(k) = \Sigma^f(m_f) + \left.\frac{\partial \Sigma^f}{\partial \not{k}}\right|_{\not{k}=m_f} (\not{k} - m_f)\ ; \tag{G38}$$

compare with (G13). The net amplitude

$$\hat{\Sigma}^f(k) = \Sigma^f(k) - \overline{\Sigma}^f(k) \tag{G39}$$

satisfies the expected mass shell condition

$$\left.\hat{\Sigma}^f(k)\right|_{\not{k}=m_f} = 0\,. \tag{G40}$$

For the corrections shown in Fig. 11, we have [67]

$$\Sigma^f(k) = \not{k}\Sigma_V^f\left(k^2\right) + \not{k}\gamma_5\Sigma_A^f\left(k^2\right) + m_f\Sigma_S^f\left(k^2\right)\ , \tag{G41}$$

where

$$\begin{aligned}\Sigma_V^f \;=\; & -\frac{\alpha}{4\pi}\left\{Q_f^2\left[2B_1\left(k^2; m_f, \mu\right) + 1\right] + \left(v_f^2 + a_f^2\right)\left[2B_1\left(k^2; m_f, m_Z\right) + 1\right]\right. \\ & \left. + \frac{1}{4s_w^2}\left[2B_1\left(k^2; m_f, m_W\right) + 1\right]\right\}\ ,\end{aligned}$$

$$\Sigma_A^f \;=\; -\frac{\alpha}{4\pi}\left\{2v_f a_f\left[2B_1\left(k^2; m_f, m_Z\right) + 1\right] - \frac{1}{4s_w^2}\left[2B_1\left(k^2; m_{f'}, m_W\right) + 1\right]\right\}\ , \text{ and}$$

$$\Sigma_S^f \;=\; -\frac{\alpha}{4\pi}\left\{Q_f^2\left[4B_\circ\left(k^2; m_f, \mu\right) - 2\right] + \left(v_{i\sigma}^2 - a_{i\sigma}^2\right)\left[4B_\circ\left(k^2; m_f, m_Z\right) - 2\right]\right\}\ .$$

Substituting vector $\left(V = \not{k}\Sigma_V^f\right)$, axial $\left(A = \not{k}\gamma_5\Sigma_A^f\right)$, and scalar $\left(S = m_f\Sigma_S^f\right)$ parts of equation (G41) into (G38), we obtain

$$\overline{\Sigma}^f(k) = \overline{V}(k) + \overline{A}(k) + \overline{S}(k)\ , \tag{G42}$$

where

$$\begin{aligned}
\overline{V} &= \not{k}\Sigma_V^f\left(m^2\right) + 2m_f^2\left.\frac{\partial\Sigma_V^f}{\partial k^2}\right|_{k^2=m_f^2}\left(\not{k}-m_f\right)\ ,\\
\overline{A} &= -\gamma_5\not{k}\Sigma_A^f\left(m_f^2\right)\ ,\ \text{and}\\
\overline{S} &= m_f\Sigma_S^f\left(m^2\right) + 2m_f^2\left.\frac{\partial\Sigma_S^f}{\partial k^2}\right|_{k^2=m_f^2}\left(\not{k}-m_f\right)\ .
\end{aligned}$$

The identity

$$\frac{\partial\Sigma_J^f}{\partial\not{k}} = 2\not{k}\frac{\partial\Sigma_J^f}{\partial k^2} \tag{G43}$$

has been used to evaluate derivatives for $J = \{V,\, A,\, S\}$. For the derivative of A, we have replaced $-\not{k}\gamma_5 = \gamma_5\not{k}$ so $\not{k}$ stands to the right as required by equation (G38); one finds

$$\frac{\partial\overline{A}}{\partial\not{k}} = -\gamma_5\Sigma_A^f\,, \tag{G44}$$

where the symmetrized expression for the derivative

$$\begin{aligned}
\frac{\partial}{\partial\not{k}}\left[\gamma_5\Sigma_A^f\right] &= \frac{1}{2}\frac{\partial}{\partial\not{k}}\left[\gamma_5\Sigma_A^f + \Sigma_A^f\gamma_5\right] \\
&= \frac{\partial\Sigma_A^f}{\partial k^2}\left(\gamma_5\not{k} + \not{k}\gamma_5\right) = 0
\end{aligned} \tag{G45}$$

has also been employed. Collecting terms, the net amplitude (G39) reduces to

$$\hat{\Sigma}^f\left(k\right) = \not{k}\hat{\Sigma}_V\left(k^2\right) + \not{k}\gamma_5\hat{\Sigma}_A\left(k^2\right) + m_f\hat{\Sigma}_S\left(k^2\right)\ , \tag{G46}$$

where

$$\begin{aligned}
\hat{\Sigma}_V\left(k^2\right) &= \Sigma_V^f\left(k^2\right) - \Sigma_V^f\left(m_f^2\right) - 2m_f^2\left.\frac{\partial\Sigma_{VS}^f}{\partial k^2}\right|_{k^2=m_f^2}\ ,\\
\hat{\Sigma}_A\left(k^2\right) &= \Sigma_A^f\left(k^2\right) - \Sigma_A^f\left(m_f^2\right)\ ,\\
\hat{\Sigma}_S\left(k^2\right) &= \Sigma_S^f\left(k^2\right) - \Sigma_S^f\left(m_f^2\right) + 2m_f^2\left.\frac{\partial\Sigma_{VS}^f}{\partial k^2}\right|_{k^2=m_f^2}\ ,
\end{aligned}$$

and $\Sigma_{VS}^f = \Sigma_V^f + \Sigma_S^f$.

Using formulae in [43, 67], the renormalization constants are

$$\begin{aligned}
\delta Z_V &= -\Sigma_V^f\left(m_f^2\right) - 2m_f^2\left.\frac{\partial\Sigma_{VS}^f}{\partial k^2}\right|_{k^2=m_f^2}\ ,\\
\delta Z_A &= \Sigma_A^f\left(m_f^2\right)\ ,\\
\delta m_f &= m_f\Sigma_S^f\left(m_f^2\right)\ ,
\end{aligned}$$

and it can be seen that the result (G46) agrees precisely with that obtained from renormalization. Numerical results for fermion self-energy functions for an electron are given in Appendix G 6: Fig. 17.

3. Vertex corrections

Consider the vertex corrections shown in Fig. 12; in the small fermion mass limit [82], only vector and axial vector terms contribute, and the core amplitude is

$$\Lambda_\mu^{\gamma f}\left(k^2, m_f\right) = \gamma_\mu\Lambda_V^{\gamma f}\left(k^2, m_f\right) - \gamma_\mu\gamma_5\Lambda_A^{\gamma f}\left(k^2, m_f\right)\ , \tag{G47}$$

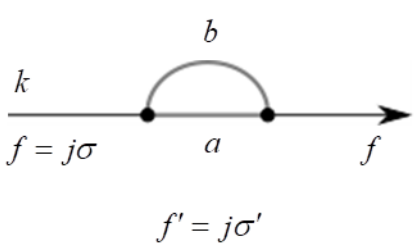

a	b
f	γ
f	Z
f′	W^+
f′	ϕ^+

Figure 11. Fermion self-energy.

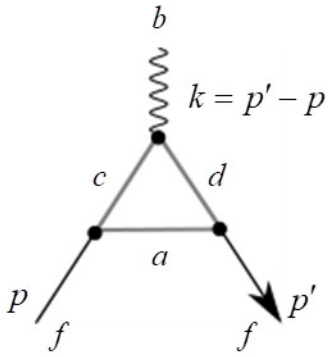

a	b	c	d
γ	γ	f	f
Z	γ	f	f
γ	Z	f	f
Z	Z	f	f
W^+	γ	f′	f′
f′	Z	W^-	W^+
ϕ^+	γ	f′	f′
f′	γ	ϕ^-	ϕ^+
f′	γ	ϕ^-	W^+
f′	γ	W^-	ϕ^+

Figure 12. Vertex corrections.

where $k^2 = (p' - p)^2$. The functions

$$\Lambda^{\gamma f}_{V,A}\left(k^2, m_f\right) = \Lambda^{\gamma f}_{V,A}\left(0, m_f\right) + F^{\gamma f}_{V,A}\left(\frac{k^2}{m_f^2}\right) \tag{G48}$$

involve singular parts at $k^2 = 0$ and finite form factors $F^{\gamma f}_{V,A}$ which vanish at $k^2 = 0$. Detailed expressions for the functions are given in [43]. Applying equation (21) with (22), dressed form factors in equation (G48) vanish as $\eta \to \infty$ in

$$m_f\left(\eta\right) = m_f\left(1 + \lambda\eta\right) \ ;$$

therefore,

$$\overline{\Lambda}^{\gamma f}_{\mu} = \gamma_\mu \Lambda^{\gamma f}_{V}\left(0, m_f\right) - \gamma_\mu\gamma_5 \Lambda^{\gamma f}_{A}\left(0, m_f\right) \ , \tag{G49}$$

and the net vertex amplitude from equation (20) reduces to the expected result from renormalization

$$\hat{\Lambda}^{\gamma f}_{\mu} = \gamma_\mu F^{\gamma f}_{V}\left(\frac{k^2}{m_f^2}\right) - \gamma_\mu\gamma_5 F^{\gamma f}_{A}\left(\frac{k^2}{m_f^2}\right) \ . \tag{G50}$$

4. Wave field renormalization and Δr corrections

In the stabilized theory, Δr factors for $\{W,\, Z\}$ follow easily from the constancy of the electrical charge; squaring equation (C23) and taking variations, we have

$$\begin{aligned} \delta e^2 &= \delta g_W^2 s_w^2 + g_W^2 \delta s_w^2 = 0\,, & \text{(G51)} \\ &= \delta g_B^2 c_w^2 + g_B^2 \delta c_w^2 = 0\,. & \text{(G52)} \end{aligned}$$

Employing equation (C10), the quadratic coupling deltas are

$$\delta g_W^2 = -g_W^2 \Delta r^W\,, \tag{G53}$$

$$\begin{aligned} \delta g_Z^2 &= \delta g_W^2 + \delta g_B^2 & \text{(G54)} \\ &= -g_Z^2 \Delta r^Z\,, \end{aligned}$$

where

$$\delta g_B^2 = g_B^2 \left(\frac{\delta m_Z^2}{m_Z^2} - \frac{\delta m_W^2}{m_W^2} \right)\,.$$

For baseline couplings g_W and g_Z, free field propagators are modified

$$\frac{1}{k^2 - m_b^2} \to \frac{1}{k^2 - m_b^2} - \frac{1}{k^2 - m_b^2} \hat{\Sigma}^b \left(k^2\right) \frac{1}{k^2 - m_b^2} \quad (b = W,\, Z)\,. \tag{G55}$$

to include diagrams in Figs. 9 and 10. Accounting for coupling changes in equations (G53) and (G54) leads to small departures of the propagator residue from unity according to

$$g_b \bullet\!\!\sim\!\!\sim\!\!\bullet g_b = \frac{g_b^2}{k^2 - m_b^2} \to g_b^2 \frac{1 - \Delta r^b}{k^2 - m_b^2} \tag{G56}$$

which results in a replacement

$$\hat{\Sigma}^b \left(k^2\right) \to \hat{\Sigma}^b \left(k^2\right) + \left(k^2 - m_b^2\right) \Delta r^b \tag{G57}$$

in equation (G55), where small terms of $O\left(\Delta r^b \hat{\Sigma}^b\right)$ have been omitted.

For $\gamma - Z$ mixing, Sirlin's variational method [42] yields a squared mass shift factor

$$\delta m_{\gamma Z}^2 = -\frac{1}{2} m_Z^2 \Delta r^{\gamma Z} \tag{G58}$$

in a Lagrangian density correction

$$\delta \mathcal{L}_{\gamma Z} = \delta m_{\gamma Z}^2 A_\mu Z^\mu\,. \tag{G59}$$

Taking into account equation (C13), (G58) suggests an effective coupling constant change $\delta g_{\gamma Z}^2 \equiv -g_Z^2 \Delta r^{\gamma Z}$ analogous to equations (G53) and (G54). Similarly to equations (G55) and (G56), the free field propagator is modified

$$\frac{1}{k^2 - m_Z^2} \to \frac{1 - \Delta r^{\gamma Z}}{k^2 - m_Z^2} - \frac{1}{k^2} \hat{\Sigma}^{\gamma Z} \left(k^2\right) \frac{1}{k^2 - m_Z^2} + O\left(\Delta r^{\gamma Z} \hat{\Sigma}^{\gamma Z}\right)\,,$$

and the Z–boson propagator

$$D_{\mu\nu}^Z (k) \simeq \frac{-i g_{\mu\nu}}{k^2 - m_Z^2} + \delta D_{\mu\nu}^{\gamma Z} (k) \tag{G60}$$

includes a correction for $\gamma - Z$ mixing

$$\delta D_{\mu\nu}^{\gamma Z} (k) = i g_{\mu\nu} \left\{ \frac{1}{k^2} \left[\hat{\Sigma}^{\gamma Z} \left(k^2\right) + k^2 \Delta r^{\gamma Z} \right] \frac{1}{k^2 - m_Z^2} \right\} \tag{G61}$$

in agreement with (G31) and equations (3.11 and 3.23) in [43].

Alternatively, standard renormalization theory (SRT) introduces mass and wave field renormalization constants to construct finite S-matrix elements and Green's functions. Renormalized amplitudes are given by [43]

$$\hat{\Sigma}^{\gamma}_{ra}\left(k^2,\,\Pi^{\gamma}\right) \;=\; \Sigma^{\gamma}\left(k^2\right)+k^2\delta Z_{\gamma}\equiv k^2\left[\Pi^{\gamma}\left(k^2\right)+\delta Z_{\gamma}\right]\,, \tag{G62}$$

$$\hat{\Sigma}^{\gamma Z}_{ra}\left(k^2,\,\Sigma^{\gamma Z}\right) \;=\; \Sigma^{\gamma Z}\left(k^2\right)+\frac{1}{2}\left[\delta Z_{\gamma Z}k^2+\delta Z_{Z\gamma}\left(k^2-m_Z^2\right)\right]\,, \tag{G63}$$

$$\hat{\Sigma}^{Z}_{ra}\left(k^2,\,\Sigma^{Z}\right) \;=\; \Sigma^{Z}\left(k^2\right)-\delta M_Z^2+\delta Z_Z\left(k^2-m_Z^2\right)\,, \tag{G64}$$

$$\hat{\Sigma}^{W}_{ra}\left(k^2,\,\Sigma^{W}\right) \;=\; \Sigma^{W}\left(k^2\right)-\delta M_W^2+\delta Z_W\left(k^2-m_W^2\right)\,, \tag{G65}$$

where δZ_Z and δZ_W are displacements of field renormalization constants

$$Z_b=1+\delta Z_b\;\;(b=Z,W)$$

from unity, and $\{\delta Z_{Z\gamma},\,\delta Z_{\gamma Z}\}$ define a correction to the $\gamma-Z$ mixing propagator [85]

$$\delta D^{\gamma Z}_{\mu\nu}\left(k\right) \;=\; ig_{\mu\nu}\left\{\frac{1}{2}\left(\frac{\delta Z_{Z\gamma}}{k^2}+\frac{\delta Z_{\gamma Z}}{k^2-m_Z^2}\right)+\frac{1}{k^2}\Sigma^{\gamma Z}\left(k^2\right)\frac{1}{k^2-m_Z^2}\right\}\,. \tag{G66}$$

From field renormalization relations

$$W_{\circ\mu} \;=\; \left[Z_W^{1/2}\simeq 1+\frac{1}{2}\delta Z_W\right]W_{\mu}\,, \tag{G67}$$

$$B_{\circ\mu} \;=\; \left[Z_B^{1/2}\simeq 1+\frac{1}{2}\delta Z_B\right]B_{\mu}\,, \tag{G68}$$

and (C9), the physical fields satisfy

$$\left[\begin{array}{c} Z_{\circ\mu}\\ A_{\circ\mu}\end{array}\right]=\left[\begin{array}{cc} 1+\frac{1}{2}\delta Z_Z & \frac{1}{2}\delta Z_{Z\gamma}\\ \frac{1}{2}\delta Z_{\gamma Z} & 1+\frac{1}{2}\delta Z_{\gamma}\end{array}\right]\left[\begin{array}{c} Z_{\mu}\\ A_{\mu}\end{array}\right]\,, \tag{G69}$$

where subscripts '$\circ$' denote bare quantities, and renormalization constants satisfy [84]

$$\begin{aligned}\left[\begin{array}{c}\delta Z_Z\\ \delta Z_{\gamma}\end{array}\right] \;&=\; \left[\begin{array}{cc} c_w^2 & s_w^2\\ s_w^2 & c_w^2\end{array}\right]\left[\begin{array}{c}\delta Z_W\\ \delta Z_B\end{array}\right]\,,\\ \delta Z_{Z\gamma} \;&=\; -s_wc_w\left(\delta Z_W-\delta Z_B\right)-\Delta r^{\gamma Z}\,,\text{ and}\\ \delta Z_{\gamma Z} \;&=\; -s_wc_w\left(\delta Z_W-\delta Z_B\right)+\Delta r^{\gamma Z}\,.\end{aligned}$$

Ordinarily, core amplitudes Σ^b are used in equations (G62)-(G65); however, with the stabilized amplitudes at our disposal, we are free to replace Σ^b with $\hat{\Sigma}^b_{sa}=\hat{\Sigma}^b$ from (G18) to more easily determine the constants. Applying mass shell stability conditions

$$\left[\begin{array}{c}\hat{\Pi}^{\gamma}_{ra}\left(0,\,\hat{\Pi}^{\gamma}_{sa}\right)\\ \hat{\Sigma}^{\gamma Z}_{ra}\left(0,\,\hat{\Sigma}^{\gamma Z}_{sa}\right)\\ \hat{\Sigma}^{Z}_{ra}\left(m_Z^2,\,\hat{\Sigma}^{Z}_{sa}\right)\\ \hat{\Sigma}^{W}_{ra}\left(m_W^2,\,\hat{\Sigma}^{W}_{sa}\right)\end{array}\right]=\overrightarrow{0}\,, \tag{G70}$$

only finite wave field stability corrections for Δr shown in Table I are non-zero; values for renormalization constants from SRT are included for comparison.

Referring to (G66), the stability result $\delta Z_{Z\gamma}=0$ means that the photon propagator has no Z-component

$$\frac{\delta Z_{Z\gamma}}{k^2}=0\,; \tag{G71}$$

consequently, there is no direct coupling between the photon and neutral current J_{NC} for $\gamma-Z$ mixing — not even an infinite one! On the other hand, an electromagnetic current couples to J_{NC} via the Z with amplitude [85]

$$\frac{1}{2}\delta Z_{\gamma Z}=\Delta r^{\gamma Z}\,. \tag{G72}$$

Table I. Stability and renormalization constants

Parameter	Stability	Renormalization
Σ^b	$\hat{\Sigma}^b_{sa}$	Σ^b
$\delta M_b^2 \quad (b = Z, W)$	0	$Re\left[\Sigma^b\left(m_b^2\right)\right]$
δZ_γ	0	$-\Pi^\gamma(0)$
$\delta Z_{Z\gamma}$	0	$\frac{2\Sigma^{\gamma Z}(0)}{m_Z^2}$
$\delta Z_{\gamma Z}$	$2\Delta r^{\gamma Z}$	$\frac{2\Sigma^{\gamma Z}(0)}{m_Z^2} + 2\Delta r^{\gamma Z}$
δZ_Z	Δr^Z	$-\Pi^\gamma(0) + \Delta r^Z + \frac{c_w^2 - s_w^2}{s_w c_w}\frac{2\Sigma^{\gamma Z}(0)}{m_Z^2}$
δZ_W	Δr^W	$-\Pi^\gamma(0) + \Delta r^W + \frac{c_w}{s_w}\frac{2\Sigma^{\gamma Z}(0)}{m_Z^2}$

5. Muon decay and Δr corrections

In the Born approximation, the muon decay amplitude corresponds to a Feynman diagram

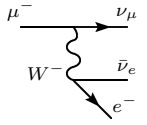

in the Standard Model. The resulting decay rate [43]

$$\Gamma_\mu^\circ = \frac{\alpha^2}{384\pi}\frac{m_\mu^5}{s_w^4 m_W^4}\left(1 - \frac{8m_e^2}{m_\mu^2}\right), \tag{G73}$$

when reconciled with the Fermi contact model prediction

$$\Gamma_\mu^F = \frac{G_F^2 m_\mu^5}{192\pi^3}\left(1 - \frac{8m_e^2}{m_\mu^2}\right), \tag{G74}$$

yields the Fermi constant in lowest order

$$G_F^\circ = \frac{\pi\alpha}{\sqrt{2}s_w^2 m_W^2}. \tag{G75}$$

With higher-order QED corrections [86, 87],

$$\frac{1}{\tau_\mu} = \frac{G_F^2 m_\mu^5}{192\pi^3} f\left(\frac{m_e^2}{m_\mu^2}\right)(1 + \Delta_{QED}) \tag{G76}$$

defines G_F in terms of the precisely measured muon lifetime τ_μ, where

$$\begin{aligned} f(x) &= 1 - 8x - 12x^2 \ln x + 8x^3 - x^4, \text{ and} \\ \Delta_{QED} &= \frac{\alpha}{2\pi}\left(\frac{25}{4} - \pi^2\right) + O\left(\alpha^2\right). \end{aligned}$$

In addition to the one-loop correction shown in Δ_{QED}, $O\left(\alpha^2\right)$ corrections for two-loops are also known [88–90]. These QED corrections involve several renormalization schemes; however, the corresponding stabilized QED corrections are finite without renormalization as shown in Appendix E. Stability corrections for vacuum polarization involve a subtraction of the form (E7) at $k^2 = 0$ and are therefore equivalent to the on-shell renormalization scheme. For other renormalization schemes; for example, the modified minimal subtraction $\overline{MS}$, Δ_{QED} involves a coupling constant renormalization. Ritbergen [88] gives a prescription

$$\alpha(m_\mu) = \frac{\alpha}{1 - \frac{\alpha}{3\pi}\ln\frac{m_\mu^2}{m_e^2}} + O\left(\alpha^3\right) \tag{G77}$$

Table II. Numerical results for Δr and derivative shifts.

Item	γ	γZ	Z	W
$m_b\left(GeV/c^2\right)$	0	$\{0,\, m_Z\}$	91.1876	80.379
$\frac{\delta m_b^2}{m_b^2}$	–	–	-0.1061	-0.0920
Δr^b	0	0.0258	-0.0329	-0.0470
$\frac{\partial \Sigma^b}{\partial s}\left(m_b^2\right)\Big\vert_{finite}$	$-\frac{\alpha}{6\pi}$	0.001165	-0.1142	-0.1252

relating the $\overline{MS}$ coupling constant $\alpha\left(m_\mu\right)$ to the on-shell (experimental) value α [69]. However, from equations (E11) and (G29), the stabilized results are unique, and (G77) does not represent an intrinsic renormalization of electrical charge in the stabilized theory.

Electroweak corrections to the muon lifetime involve Δr corrections to the Fermi constant [42, 43, 91]

$$G_F \;=\; G_F^\circ\left[1+\Delta r\right]\;, \tag{G78}$$

where after renormalization

$$\Delta r = -\Delta r^W - \frac{\delta m_W^2}{m_W^2} + \frac{\hat{\Sigma}^w\left(0\right)}{m_W^2} + \Delta r^{[\text{vertex, box}]}\;, \tag{G79}$$

$$\Delta r^{[\text{vertex, box}]} = \frac{\alpha}{4\pi s_w^2}\left(6+\frac{7-4s_w^2}{2s_w^2}\ln c_w^2\right)\;.$$

From a stability perspective, the first two terms of equation (G79) are due to finite mass shifts (G33) and (G34); taking into account equation (G29), variation of (G75) yields

$$\delta G_F^\circ \;=\; -G_F^\circ\left[\Delta r^W + \frac{\delta m_W^2}{m_W^2}\right]\;. \tag{G80}$$

In standard renormalization theory, divergent bare parameters $\{\alpha_\circ,\, s_w^\circ,\, m_w^\circ\}$ replace those in equation (G75), and the expression for Δr includes a charge renormalization term $\delta\alpha_\circ$ which is subsequently incorporated into a renormalized coupling.

6. Numerical results

Code for generating the following numerical results is provided in Ref. [92]. Values for Δr are tabulated in Table II using $\sin^2\left(\theta_W\right) = 0.23122(4)$ and other physical constants [69].

Real parts of boson polarization functions (G20) are plotted in Figs. 13–16. Stability profiles use amplitudes (G14) or, equivalently, (G18) exclusive of Δr. Results in Fig. 13 agree with those in Fig. 8 of [67] notwithstanding updated physical constants [69]; QED results are added for comparison using an analytic result for equation (E7) given in [93]. For numerical evaluation of photon self-energy and $\gamma - Z$ mixing profiles shown in Figs. 13–14, the stability value at $s = 0$ is not represented; but analytically, $\hat{\Pi}^\gamma\left(0\right) = \hat{\Pi}^{\gamma Z}\left(0\right) = 0$ from equation (G20). Differences between $'Stability + \Delta r'$ profiles shown in Figs. 14–16 and Figs. 9–11 of [67] are due to

1. Δr impacts arising from updates to $\left\{\Sigma^Z,\, \Sigma^W\right\}$ in [43] relative to [67],
2. derivative shifts in Table II, and
3. updated physical constants including a Higgs mass measurement $125.18 \pm 0.16\, GeV/c^2$ [69].

Analytic expressions for $F\left(s, m_1, m_2\right)$ given in [67] and its partials were verified against numerical integration results for all mass arguments m_1 and m_2 over the range $0 < \sqrt{|k^2|} < 200\, GeV$.

Electron self-energy function profiles $\left\{\hat{\Sigma}_V,\, \hat{\Sigma}_A,\, \hat{\Sigma}_S\right\}$ shown in Fig. 17 agree with those in Fig. 18a of [67].

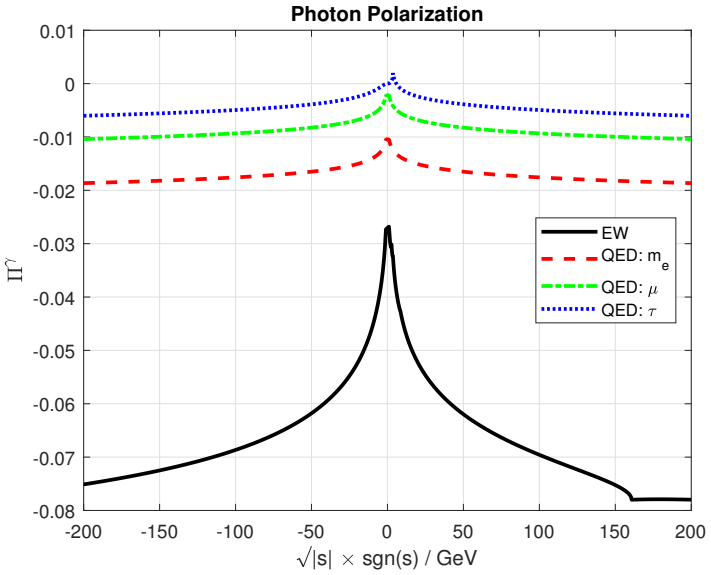

Figure 13. Stabilized electroweak photon polarization is compared with QED for electron, muon, and tau.

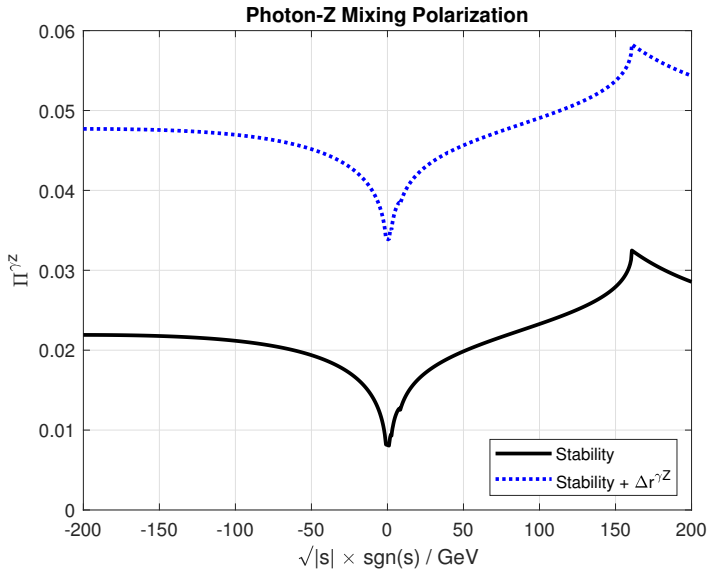

Figure 14. Stabilized photon-Z mixing profiles with/without adjustments for Δr.

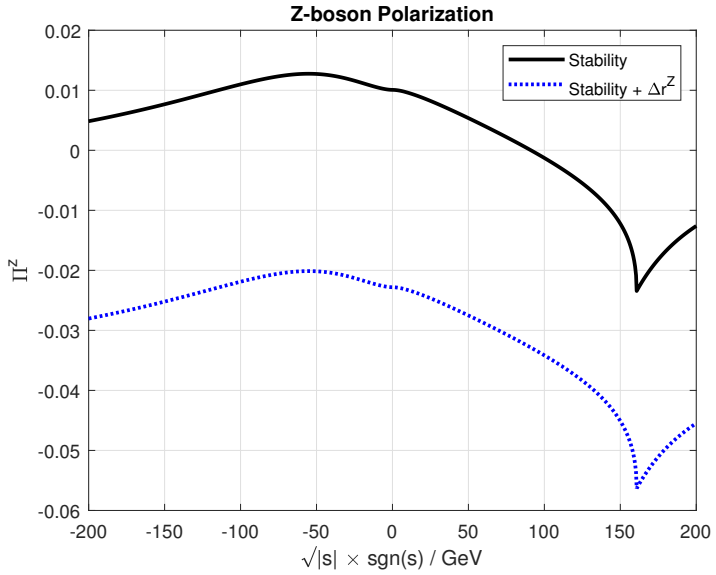

Figure 15. Stabilized Z-boson polarization profiles with/without adjustments for Δr.

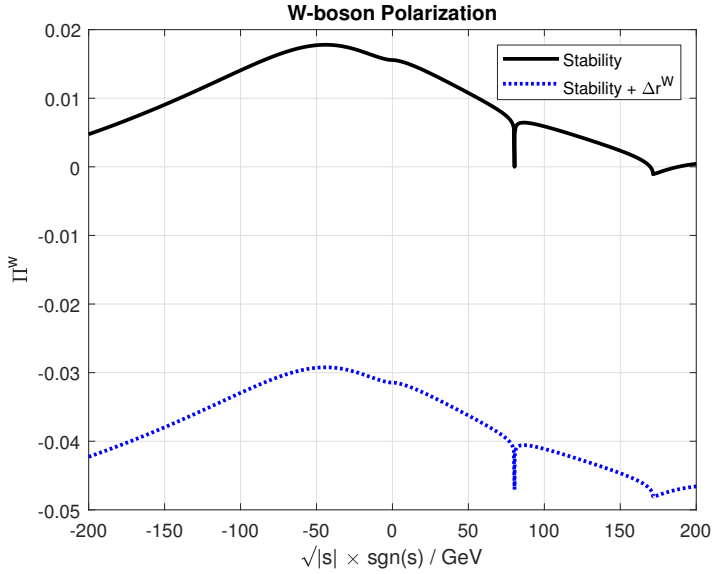

Figure 16. Stabilized W-boson polarization profiles with/without adjustments for Δr.

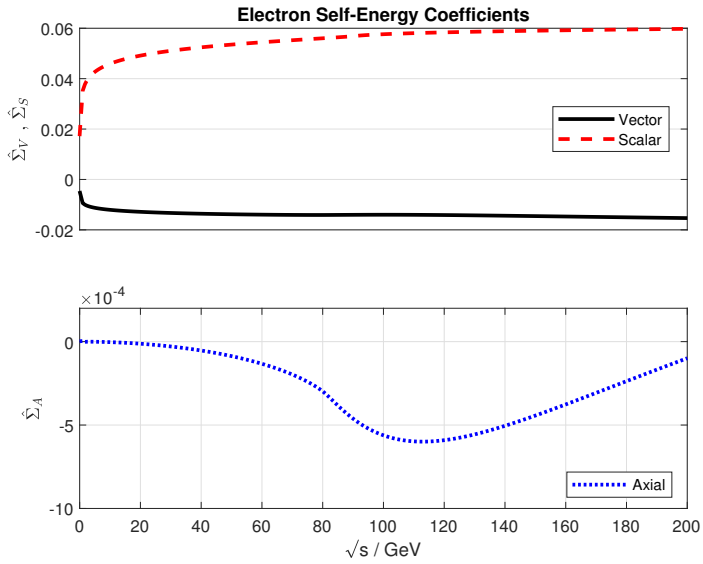

Figure 17. Electron self-energy coefficients for vector, axial, and scalar contributions.